FIRE ANTS BUILD SELF-HEALING TOWERS

A Thesis
Presented to
The Academic Faculty

by

Sulisay Phonekeo

In Partial Fulfillment
of the Requirements for the Degree
Master of Science in the
Woodruff School of Mechanical Engineering

Georgia Institute of Technology
December 2015

FIRE ANTS BUILD SELF-HEALING TOWERS

Approved by:

Professor David L. Hu, Advisor
Woodruff School of Mechanical Engineering
Georgia Institute of Technology

Professor Craig A. Tovey
School of Industrial and Systems Engineering
Georgia Institute of Technology

Professor Jonathan Rogers
Woodruff School of Mechanical Engineering
Georgia Institute of Technology

Date Approved: 24 July 2015

TABLE OF CONTENTS

LIST OF TABLES

LIST OF FIGURES

SUMMARY

This study considers the construction and preservation of structures built by fire ants, *Solenopsis Invicta*. The construction of shelter is a universal ability of living systems, and is manifested among caterpillar tents, bird nests, and primate nests. While much headway has been made into the principles of swarm behavior in bird flocks and schools of fish, less is understood about how systems can self-assemble to build temporary shelters. This study uses videography to show how fire ants can build structures much larger than themselves: by designing structures of particular shape and using the ability to self-heal to preserve the structures. We used micro scale observations to predict the construction of fire ant towers and conducted material testing on fire ant aggregate to quantify their physical properties. In addition, we compare ant aggregates to cell aggregates to develop common experimental methods to study the collective motion of these self-assemblages. The mechanisms and rules found here may contribute to the studies of both living and robotic swarms.

CHAPTER I

INTRODUCTION

1.1 Motivation

Organisms have evolved many ways to self-assemble for survival. Skins cells can signal for repair of wounds[8,9], Dictyostelium slime mold cells can self-assemble to increase likelihood of finding food[10] and insects can collectively self-assemble to form shelter and reduce obstacles. Many animals such as ants, fish, bees and birds exhibit swarm behavior which also incorporates collective aggregation and self-assembly. This strength in numbers has allowed these animals to avoid predation. Insects, in particular, use strength in numbers for their benefit when self-assembly to build shelters[11].

The cooperative behavior of animals has gathered much interests due to potential applications of decentralized systems[12–16]. Animals such as termites and ants build structures many times their size, such as ant bivouacs and termite mounds, the latter of which which can reach 8 meters in height.[17,18]. Animals, limited by the resources and materials available to them, are still able to build various structures to fit their needs[19]. This ability to build adaptable structures is exemplified in insect society assemblages. Insects such as bees and ants have the ability to build complex structures by using very limited resources and in many cases, their bodies. Their structures can range from bridges which help cross gaps or shelters that protect the colony from the environment[11]. Bonabeau and Theraulaz modeled ants falling like dripping liquid[20,21]. Couzin demonstrated how information transfers throughout the ant colony to make collective decisions[22].

There have been many instances such where the study of ants have inspire algorithms and development of modular robots[23–26]. However, much still remains in the field of modeling collective behaviors from the interactions of the individuals. Developing effective

models of on the individual level could inspire more development in the control of hundreds of thousands of robots instead only a thousand individual[27]. A look into the way ants connect inside their aggregates has implications in the study of active matter and self-healing materials.

1.2 Background & Previous Work

1.2.1 Self-assemblages

Self-organization is an organize behavior that arises from the interactions between individuals in a large group. Individuals of varying sizes ranging from cells to insects and birds, work together to build complex structures and systems without a central leader. In the biological domain, it is common to see organisms that interact with each other following simple rules and, in spite of that, complex collective behavior and spatial-temporal structures may emerge, which are extremely difficult to predict from the individual level[28]. Such behaviors can lead to aggregations that organisms can use to accomplish complex tasks that individuals cannot perform.

On the macroscopic level, the observation of animal aggregates dates back to the 1920's[29] with observations of flocks of birds and schools fish. In the 1840's, Savage was one of the first to record the aggregations made by driver ants or army ants of Africa[30]. He observed raiding trails filled with millions of traveling driver ant the arches that larger ants form to protect the flow of smaller ants. Savage follows the raiding trial and made early observations of the adaptability of ant aggregations. In his observations, Savage noted the formation of chains that the ants form by connecting on branches to the bottom of a tree which appears to be formation of bivouacs based on his descriptions. If there is water in front of their paths, these ants would form water bridges to cross the gaps and during the frequent flooding of the rain season, these ants would throw themselves into a rounded mass and float on the water until the flood subsided or safety is reached. Since Savages study, there have been many studies that elucidate how ants are able to perform these complex

tasks. **Fig.1** show some example of assemblages by ants.

Figure 1: Ants can self-organize to build structures against gravity. (A) Ants self-organize to build bivouacs to survive above ground. (B) Ants join together to form a bridge to cross a gap (C) Ants aggregates spread across the water to make a raft. (D) Ants are very strong and uses this property to stay together as shown here by the drip of ants.

In more recent years, Anderson *et al.*gives a detailed review of different types of assemblages by insect societies[11]. The review explains the form and functions of self-assemblages, from 2D structures such as chains and curtains to 3D structures such as bivouacs and bridges. He categorizes the self-assemblages by complexities and also gave reasons for some of the functions of these structures. For example, bivouacs (temporary ant shelters) are the central control of the colony, defense against predators, and are used for thermo-regulation. Ants accomplish all of these self-assemblages without a central control. There are no leaders to give directions, but there is a feed-back system with how they communicate that they allows them to build different structures.

1.2.2 Communication

Studies show that ants use simple rules to form many of their structures such as rafts, temporary shelters, bridges, and foraging trails[11,13,20,21,28,31–37]. Since many species of ants are partially or totally blind, information from their immediate surroundings and other ants are critical for navigation through new environments. Ants are believed to use tactile sensing and sensing of pheromones to prevent separation from the group[38–40]. Information found by select individuals can dictate behaviors that in turn propagate throughout the group. Such communication enables finding shortest path to the nest and food sources, or develop traffic flows that minimize congestions[41].

Studies of Argentine ants shows the use of feed-back mechanism by that ants use to find the shortest path to their food source[42]. At first ants send foragers out in all directions and once they find a food source, they come straight back to the nest to recruit. The ones that find the closest food source will come back first due to the shorter distance. As more ants go back and forth between the food source and nest, the trail of pheromones get stronger and over time, they have found the shortest path. Other studies of ants also show that certain ant species have memory and use physical cues to navigate[43,44]. These cues help to translate the baseline stochastic behavior of individual ants towards an organized movement as a whole.

1.2.3 Connections

Several important features of the ants allow them to connect and build complex structures: polymorphism, their tarsal claws, and the adhesive pads on their legs called the arolium. The way their structures are built allows ants to interchange the building blocks, their bodies, easily with little individual specialization. **Fig.2** shows the different ways that ants connect to each other. Depending on species, some ants use their tarsal claws to create strong linkages.

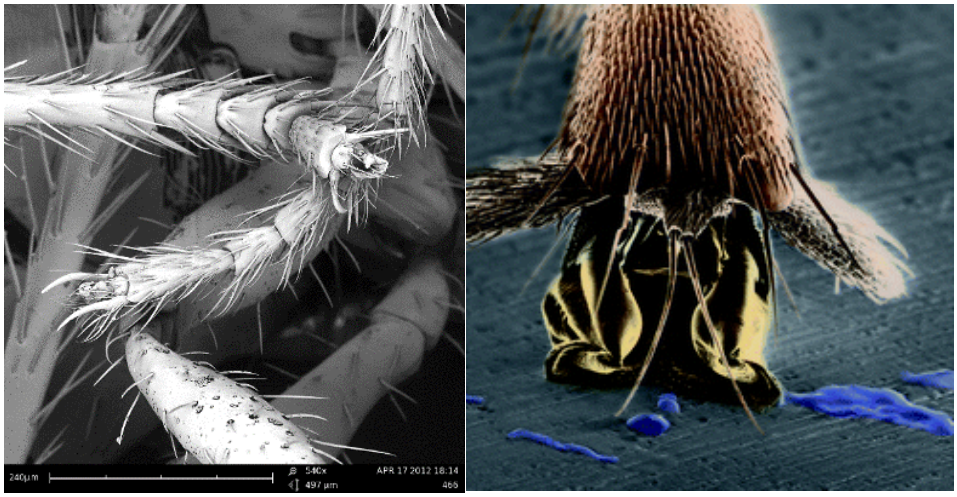

Figure 2: Hooks and sticky pads at the end of ants legs that they use to connect to each other and to substrates[1].

The arolium on the end of ant legs are very useful in making their connections and the adhesion fluid and softness of the arolium enable ants to walk against gravity and unsteady surfaces. Federle *et al.*shows that ants have control over the strength of attachment by the arolium by actively contracting their muscles and passively by the movements of their legs[45]. This physical tool, along with their small size and lack of inertia, direction of travel does not affect the motion or metabolic rate of an ant[46–48]. An ant expends as much energy per step as it moves along a floor, up a wall, or across a ceiling. Thus, ant are able to make connection to each other or other substrate in almost any environment.

More recently, Foster *et al.*delve inside ant aggregation to look at how they connect with each other. Foster *et al.*put a frozen a ball of ants inside a micro-CT scanner and found that when in aggregates, ant linkages become a complex network. Ants inside aggregates have an average of 4.8 neighbors and 8.5 connections which is contributed mostly by the leg connections and very little number of connections using the mandibles[49]. They use these leg connections to control their spacing and orient themselves relative to their neighbors.

This strategy allows the ants to react to change in their environments such increasing more air pockets inside to be more buoyant during flooding.

1.2.4 Entangled Active Matter

Studies of fire ant connections can have implications in the fields of granular media and active matter. Connections of fire ants in aggregates can be visualized by granular *u*-shape particles, such as staples. The bent legs of staples are entangled which helps to stabilize the structure and resist both compressional and extensional forces[50]. A recent study of granular *u*-shape particles by Franklin *et al.*shows staples rearrange when they are undergo extension[51]. During extension, the the force curve shows many peaks which is synonymous to connections breaking and then rearranging so the bulk material remains. The study discusses a model that is able to predict when a connection will break. However, staples connections are passive not active. Ants can control their entanglement state by using their tarsal claws and adhesive pads on their legs. They can also provide forces to oppose external disturbances in all direction due the the 3D networks they create.

Entangled active matter are non-equilibrium systems that takes in energy and collectively generate motion, has received less attention than free active matter, but provides new avenues for understanding how swarms work. Entanglement involves many individuals that are bonded to each other by transient, as in long polymer chains. These links cause entangled active matter to be found in the form of three-dimensional aggregates, such as balls of cells or ants. Moreover, the transient nature of the links can lead to a variety of behaviors. Aggregates of cells and ants exhibit viscoelasticity: at shorter time, aggregates are elastic under compression and relax like a rubber[4,5]. At longer time, they are viscous and flow like honey. Thus, living aggregates can be characterized by material properties that have only been seen up to now in inanimate materials. By characterizing these bulk material properties, we can obtain insight into the individual level of cooperation.

CHAPTER II

FIRE ANTS PERPETUALLY CIRCULATE THROUGH THEIR TOWERS OF CONSTANT STRENGTH

2.1 Introduction

This study is part of the body of research that embeds fine scale observation of individual behaviors into mathematical models to make testable predictions about the macro-scale behavior of the group. In previous work, Mlot *et al.*[6,52] built a predictive model for the rate and shape of fire ant raft construction based on observations of ant behavior atop and on the edges of the raft. This work builds on that and tries to explain the mechanisms involved in tower building by fire ants which allows them to temporary survive above ground.

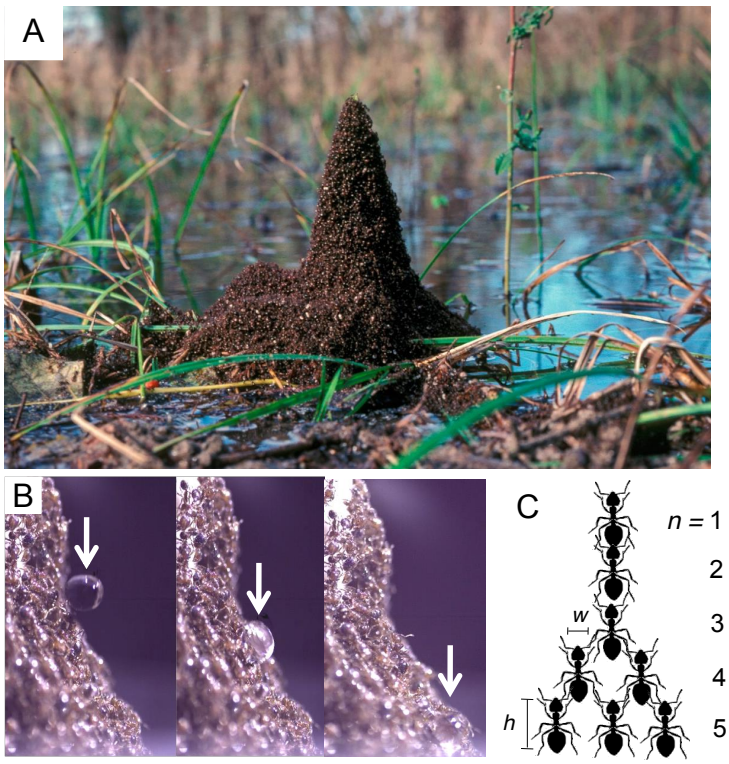

Figure 3: The shape of an ant tower. (A) A trumpet-shaped ant tower built around a small branch in the Atchafalaya Basin Swamp in Louisiana. Photo courtesy of CC Lockwood. (B) Water droplet rolling off the side of an ant tower. (C) Schematic of five layers of an ant tower with carrying capacity $\alpha = 2$ ants.

Fire ants build towers around a central support to anchor at a plant in water or as a bivouac on land when not in the nest (**Fig.3A**). They need to build these towers to have a temporary form of shelter while the colony searches for a suitable nest. Preliminary observations suggest that the towers tend to be trumpet-shaped, but the reasons for this shape remain a mystery. While the tower is being built and after it is complete, ants move in all directions on its surface, but eggs and larvae are not visible on the surface. Preliminary observations in the laboratory are consistent with these characteristics. In addition, we observe that the tower repels falling water droplets. **Fig.3B** shows a drop of water gliding along the tower surface. We also observe that the ants take an order of magnitude more time to build a tower than to spread out into a pancake-shaped raft, approximately twenty minutes compared with one to three minutes[6]. Our initial questions are, why are the towers

trumpet-shaped, how do the ants build them consistently, and why is the building time so long? From an evolutionary point of view, water repellence partially addresses the first question, and the lesser urgency to build a bivouac when traveling than to form a raft at the onset of a flood addresses the third. However, selection pressures do not elucidate the mechanisms that are in operation.

We begin by swirling 10 grams of ants ($\sim$ 10,000 ants) in a beaker to create a ball of ants. The ball is placed into the center of an acrylic box and gently pierced at the center with a Teflon rod, rendered nearly frictionless by a light coating of baby powder. The central rod prevents swaying of the ant tower, but otherwise does not support the tower's weight, which is accomplished by the ants themselves. We coat the acrylic walls with Fluon to dissuade building on the walls of the container. At the beginning of the experiment, ants explore and try to build over the walls, but eventually they focus their efforts on the central Teflon rod (see movie **S1**).

2.2 Methods

Ant husbandry

We procure ant colonies from roadsides near Atlanta, GA. Colony selection aims for an average ant weight of 1 mg. We remove colonies from the soil and place them into bins according to methods by Chen[53]. Ants are fed baby food and pet food 3-4 times a week and we perform experiments using 9 different colonies with regularly replenishment of their water supply.

Tower building

We collect 10 g of ants in a beaker and then swirl them to produce a ball of ants. This ball is placed in the center of a 150x150x15 mm acrylic box. We lightly dust a Teflon rod with talc powder and lower it into the center of a sea of ants filling the box. We prevent ants from escaping the sides of the box by coating the box with Fluon and talc powder on the sides. Within a few minutes ants begin to form a tower centered around the Teflon rod.

For our set of data it takes 19.5 ± 7.3 minutes for all of the ants form a stable, roughly axisymmetric tower in equilibrium around the rod. We film the process from the side to capture the tower profile. We use transparent container and a high-definition Sony HDR-HC9 video camera to capture the tunneling process. After the tower reaches equilibrium, we put the ants back in their bins for at least 2 hours before using them again. We use the same ants at most twice per day. We performed experiments using 9 different colonies and kept room temperatures between 23°-25° Celsius.

Mathematical model for tower shape

In order to model the shape, we treat the tower as consisting of horizontal layers of ants. Layer 1 is the top layer, and layer $n+1$ is immediately below layer n. Suppose one ant has a carrying capacity of α ants. Ants are known to be strong, so α will be larger than 1. Let X_n be the number of ants in layer n. The ants in layer $n+1$ must be able to support the ants in layers 1 through n. Therefore,

$$\alpha X_{n+1} \geq \sum_{i=1}^{n} X_i. \tag{2.1}$$

At maximum load, equation 2.1 will hold with equality. Hence at maximum load, it is a good approximation to write

$$\alpha X_{n+1} = \sum_{i=1}^{n} X_i = X_n + \sum_{i=1}^{n-1} X_i = X_n + \alpha X_n = X_n(\alpha + 1). \tag{2.2}$$

Equivalently,

$$X_{n+1} = X_n(1 + 1/\alpha). \tag{2.3}$$

From equation 2.3 we write the precise formula for X_{n+1} which is

$$X_{n+1} = \lceil \frac{1}{\alpha} \sum_{i=1}^{n} X_i \rceil. \tag{2.4}$$

Assuming the number of ants in the top layer, $X_1 = \beta$, and carrying capacity, $\alpha \geq 1$, we

will approximate X_n by the formula:

$$X_n = \begin{cases} \beta & \text{if } 1 \leq n \leq \alpha \\ \beta(1+1/\alpha)^{n-\alpha} & \text{if } n > \alpha \end{cases} \tag{2.5}$$

Mathematical model for tower dynamics

Let Y be a random variable for the time t it takes an ant to fill any space in a ring. We assume Y is exponentially distributed, with a cumulative distribution function (CDF) of

$$P(Y \leq t) = 1 - e^{-t/\lambda}, \text{ where } t \geq 0, \tag{2.6}$$

and λ is the mean time to fill an empty slot. Let S be the total number of spaces around a rod with diameter D. Based on an ant width of w = 1 mm, we have $S \approx \pi D/w$. When S spaces are empty, the time Z until $S-1$ spaces are empty is

$$Z = \min_{1 \leq j \leq S}(Y_j), \tag{2.7}$$

where the Y_j are jointly independent exponentially distributed variables each with mean λ. Therefore, the time Z to fill the first space is distributed so that

$$P(Z \geq t) = P(\bigcap_{j}^{S} Y_j \geq t) = \prod_{j=1}^{S} P(Y_j \geq t) = (e^{-t/\lambda})^S = e^{-t/(\lambda/S)}. \tag{2.8}$$

Therefore, Z has exponential distribution with mean λ/S. Once one space is filled, by the memoryless property, the remaining time until all the spaces are filled is the same as if we start with $S-1$ empty spaces which is equal to $\lambda/(S-1)$ plus the time as if we start with $S-2$ empty spaces. Inductively, the expected time T to fill all S empty spaces is

$$T = \sum_{j=1}^{S} \frac{\lambda}{S-j+1} = \lambda(1+1/2+1/3+\cdots+1/S) \approx \lambda \log S \tag{2.9}$$

Measurement of ant attachment strength

Ants can attach to each other and substrates by using the hooks and sticky pads on their feet[47,54,55]. We measure the strength of an ant's leg-to-leg connection by tying two ants of the same colony each to an elastic string. We place the two ants in contact to stimulate a leg-to-leg connection. Once the ants grip each other's legs, we pull the inelastic string which causes it to stretch. We then use Hooke's Law to measure the force.

We measure the force with which an ant holds to Teflon by placing Teflon rods of diameters 4.7mm (N=9), 12.8mm (N=10), and 14.5mm (N=6) on a Metler Toledo analytical balance. We place one tethered ant on the Teflon rod and slowly pull the ant upwards until it releases its hold. We record the whole process using a Sony HDR-HC9 video camera and use Tracker to find the maximum amount by which the measured weight decrease. The mean and standard deviation for all trials (N=25) were 2.56 and 1.04 dynes, respectively. The decrease in attachment strength with increasing rod diameter is noticeable: the means are 3.68 ($\sigma = 1.23$), 2.94 ($\sigma = 0.65$), and 1.70 ($\sigma = 0.63$) dynes, respectively for rods of diameter 4.7 mm, 12.8 mm, and 14.5 mm.

Tower sinking

To observe ant movement within the tower, we doped 5 g of fire ants with a radiographic contrast medium (GE Omnipaque Ioxehol solution) by mixing it with their drinking water and allowing the ants to drink for at least 2 days before building a tower. Immediately before tower building begins, we mix 5 g (5000 ants) of doped ants thoroughly with 5 g (5000 ants) of undoped ants from the same colony. In total, we used the same amount of ants as our other experiments. We placed the ants in a 100mm diameter x 55 mm tall container with an 8 mm diameter Teflon rod located in the center of the dish. We allowed the ants to build a tower with the process captured using an imaging system that includes the following: Spelman XRB502 Monoblock X-Ray source and Amorphous Silicon Digital X-Ray Detector PaxScan 2020+ (Varian Medical Systems). We operated the x-ray at a current

of 2.5 mA and a voltage of 100 keV. In the resulting images, doped ants show as dark spots, and we use "Tracker", a free product of Open Source Physics. This program allows us to trace individual paths (dark spots) of ants frame-by-frame throughout the sinking process in which we use the distance traveled by the ants over time to calculate the sinking rates.

2.3 Results

2.3.1 Shape model

Regardless tower height and size of central rod, the tower qualitatively has the same radially symmetric trumpet-shape. In our 26 experiments, tower heights range from 7 to 30 mm with an average height of 15.8 ± 5.3 mm. To explain the shape, we idealize the tower as consisting of one-ant-thick horizontal annuli around a core of rod radius D as shown **Fig.3C**. The number of ants in a layer are extrapolated from the profile of the tower. We non-dimensionalize the height and diameter of the tower using an ant standing vertically of height $h = 3$ mm and ant width $w = 1$ mm. Filming the towers from the side, we use image analysis to discretize the tower into a series of n horizontal annuli around the central rod. We hypothesize that each ant supports an equal amount of weight, analogous to the "Towers of constant strength" proposed by Timoshenko in 1930[56] and used in design of the Eiffel tower . Applying the equal-weight hypothesis to the idealized layers of the tower implies that each layer supports all of the layers above it and the weight is distributed uniformly within each layer. We introduce two parameters to characterize the shape of the tower, which we use to match the model to the experimental data. The spread of the tower is given by the ant carrying capacity α, given in ant-weights. The second parameter is the number of ants, β, in the first layer of the tower, a boundary condition that is tower-specific. We define X_n to be the number of ants in the nth layer, counting from the top layer at $n = 1$. Then

$$X_{n+1} = X_n + \lceil \frac{1}{\alpha} X_n \rceil, \tag{2.10}$$

because the $n+1$st layer needs X_n ants to support layers 1 to $n-1$ plus an additional X_n/α ants to support layer n. We assume towers are built as tall as possible and in Methods, we derive the following approximation:

$$X_n = \begin{cases} \beta & \text{if } 1 \leq n \leq \alpha \\ \beta(1+1/\alpha)^{n-\alpha} & \text{if } n > \alpha \end{cases} \tag{2.11}$$

Equation 2.11 predicts that the shape of the top portion of the tower remains the same regardless of the total tower height. This prediction will be crucial to our model of tower growth in the next section.

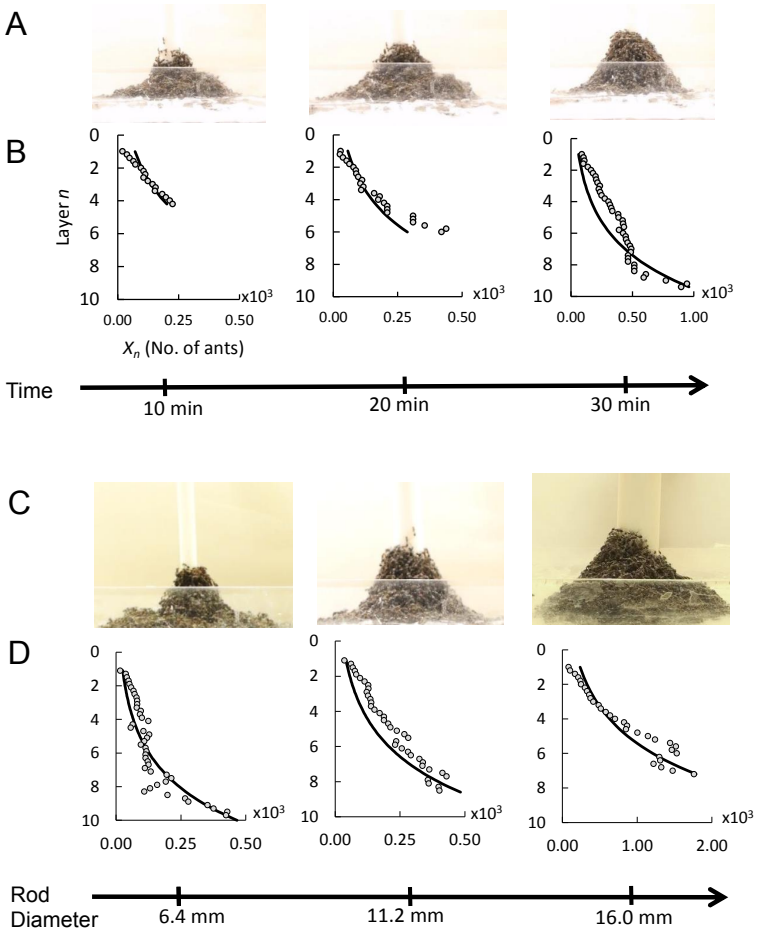

Figure 4: Ant tower profile. (A) A time sequence of an ant tower built on an 8-mm diameter Teflon Rod. (B) The fit of the shape model to the profile of a 10 min, 20 min, and equilibrium ant tower. (C) The equilibrium shape of ant towers built on 6.4-mm, 11.2-mm and 16.0-mm rod diameters. (D) The fit of the shape model the profile of the equilibrium ant towers on increasing rod diameters. The circles represent the profiles of the towers. We fit these profiles to the shape model, shown by the solid lines, using carrying capacity $\alpha = 2.6$. X_n is the number of ants in layer n, measured from the top where $X_1 = \beta$, which is tower specific.

We require the shape model to use the same value of α for all rod diameters for parsimony and because we doubt that ants not adjacent to the rod can sense its diameter. Using the method of linear least-squares, we fit predicted tower shapes to experimental ones, throughout the building process. We fit 20 ant towers, after disregarding inchoate towers that are less than 3 layers tall, from experiments using central rod diameters ranging from 4 mm to 16 mm. We . **Fig.4A** shows the 10 minute, 20 minute, and equilibrium shapes of

the towers built around an 8 mm diameter rod. In **Fig.4B**, the circles indicate the profile of the ant towers and the line is the model. The fit is good, as shown by the R^2 values of 0.86, 0.81 and 0.84, respectively ($N = 3$). The fits of the model to the ant towers are not as good at the top of the towers as compare to the bottom. Discrepancies at the first couple of layers between the model and the data are random effects. The location of the top layer is visually ambiguous so we use the better β value of the first two layers for each ant tower. We applied this method to all the ant towers to find the best fit of $\alpha = 2.6$ ants. The shape model with this α value is accurate with $R^2 = 0.84$ (N = 20). **Fig.4C** shows the towers built on increasing central rod diameters and **Fig.4D** shows the tower profiles with the theoretical predictions. As shown, the model can accurate predict the overall shape of the tower for a range of central rods on the ant tower.

To show that ants are holding each other up and not just piling on top of each other, we compare the ant tower to dead ant pile. We first euthanized ants with liquid nitrogen and then poured them through a funnel into a petri dish. This process creates a conical shape pile in which we can measure the angle of repose, the slope of the pile relative to the horizontal. For dead ants, we measured the angle to be 36°. The dead ant pile have an angle of repose because it is only supported by friction. Unlike the dead ant pile, the tower of live ants do not have an angle of repose due to the exponential shape of the tower. Therefore, this shows that ants are physically exerting themselves when in the tower rather than piling on top of each other. The value $\alpha = 2.6$ is fairly close to the value 1.5 we reported as the weight borne by ants at the bottom layer of a raft[6]. In contrast, the amount of weight required to prevent ant movement is larger by two or more orders of magnitude, demonstrated by the following compression test that we performed on three different ants with an average weight of 1.1 ± 0.15 mg . We place a 0.05-gram transparency sheet atop a single ant and gradually increase the number of sheets until the ant cannot move. Since we can observe the ants through the transparent sheets, we note when the ants stop walking in any direction. A weight of 88 ± 13 mg, or about 83 ± 12 times body weight, prevents

the ant from walking. A weight greater than 0.8 grams, or about 750 times body weight, prevents ants from moving any limbs at all but does not kill or appear to injure them after we remove the transparency sheets from the ants. These values of 83 and 750, compared with the value $\alpha = 2.6$ experienced by ants in towers, are strong evidence that ants are staying still within their towers out of their own volition, and not because of their physical limitations.

2.3.2 Shape model applies to human towers

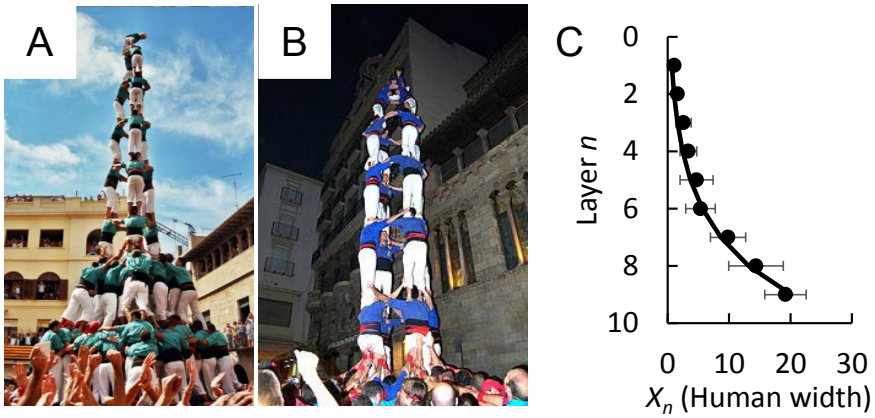

Figure 5: The shape law also shows good fit with the human towers. (A-B) Human towers built in Spain. (C) The solid circles represent the profiles of the towers found on Google, Youtube, and Wikipedia ($N = 22$ runs , yielding the errors bars shown). We fit these profiles to the shape model, shown by the solid lines, using $\beta = 1.0$ and carrying capacity $\alpha = 1.9$. Images courtesy of Eric Sala, Tània García and Montserrat Torres.

For hundreds of years, human towers have been used in siege tactics, acrobatic competitions, and rituals[57,58]. Beginning in the early 18th century, groups of Catalonians started stacking themselves together in a parade known as the "Ball del Valencians" which eventually grew into competitions to build the tallest human tower. To this day, groups of builders called Castellers still compete to build the tallest human tower, the record for which is currently 10 layers[59]. The common trends that run through all human towers are the structural tactics of building a wide base and tapering the width as the tower gets higher. We

investigate how our shape model fits these human towers. We compile Google Images and Youtube images of 22 human towers, examples of which are shown in **Fig.5A-B**. We discretize the height and width of human towers in terms of human height and width. Again, we use the method of linear least squares to estimate the carrying capacity α for the human towers. **Fig.5C** shows a plot of the human towers (circles) against the model (line). Using $\beta = 1$ and a carrying capacity $\alpha = 1.9$ yields an excellent fit with an R^2 value of 0.97. Although α for humans is similar to α for ants, ants can hold much more weight. The data from human tower profiles show that we can use our model estimate the load each person is holding similarly to what we did with ants.

2.3.3 Growth rate of tower

The shape model implies that many more ants must be added to the tower to create layer n than layer $n-1$. However, the observed rate of increase of height is fairly constant. Why doesn't it take more time to add ants of the tenth layer than the third layer? We hypothesize the following: ants follow the same rules of behavior that were observed and yielded accurate predictions about ant raft construction[6,52]. These rules are:

(1) Don't move if ants are on top of you;

(2) If atop other ants, repeatedly move a short distance in a random direction;

(3) Upon reaching available space adjacent to non-moving ants, stop and link with them.

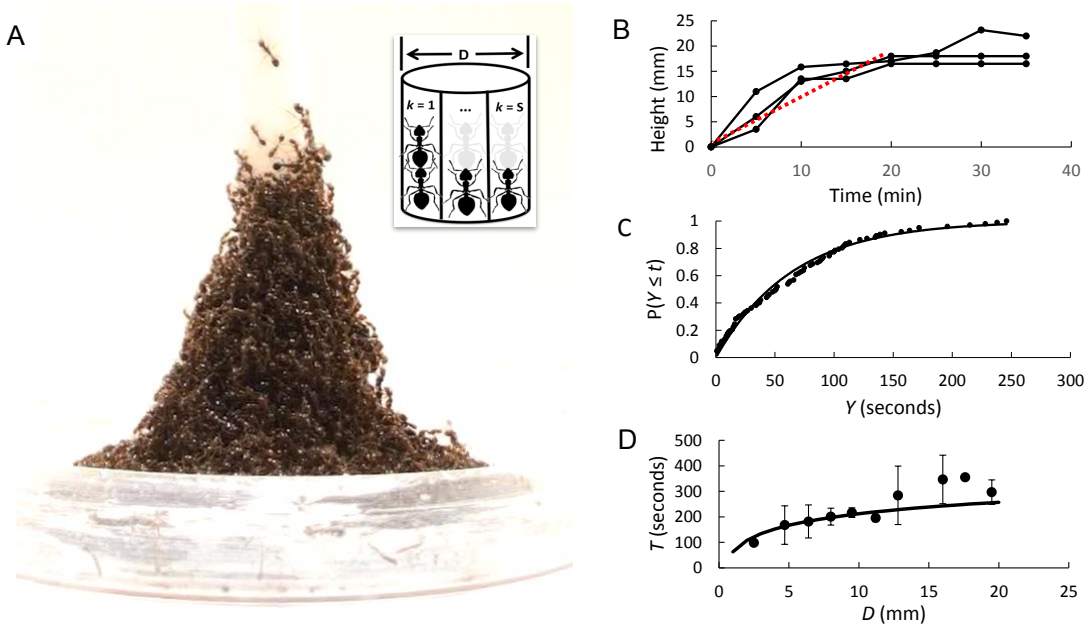

Figure 6: Building rate of ant towers. (A) A side view of an ant tower. The inset shows a ring of spaces from $k = 1$ to $k = S$ around a rod of diameter D that ants can fill. (B) Time sequence of tower height (N = 3, rod diameter = 9 mm). The red dashed line is the average growth rate. (C) The solid circles shows empirical cumulative distribution function (CDF) of the time Y to fill a slot, found from video tracking. The solid line is the CDF from the predicted exponential distribution. (D) Relationship between ring filling time and rod diameter. The circles represent the experimental time to complete a ring (N = 3 for each diameter for which an error bar is shown). The line is the predicted time to fill a ring.

The accompanying movie **S2** illustrates rules 1 and 2: many ants move up, down, and sideways seemingly at random on the tower surface; ants below the surface do not appear to move. In the case of the tower, the only available space for growth is the rod surface just above the top layer as shown in **Fig.6A**. The hypotheses together with the shape model can explain why the height grows at a constant rate as shown in **Fig.6B**. Because of rule 2, the only ants that have a chance to increase the tower's height are those in the top couple of centimeters of the tower. By the shape model, the top portion of the tower always has the same shape and size.

The inset in **Fig.6A** depicts the discretization the top of the tower into a ring of spaces.

Given that the individual ant movements are random, the time to fill an empty space on a ring should be independent of the fill time of other spaces, and have a memoryless distribution. That is, if after t seconds a space has not been filled, its remaining expected time to fill is the same as it was at zero seconds. In terms of the random variable Y equal to the time to fill a space, $E[Y|Y \geq t] = E[Y]$ for all $t \geq 0$. The exponential distribution[60] is the unique memoryless continuous distribution on the nonnegative real numbers, with cumulative distribution function (CDF)

$$P(Y \leq t) = 1 - e^{-t/\lambda}, \text{ where } t \geq 0, \tag{2.12}$$

where λ is the mean time to fill an empty space. **Fig.6C** compares the cumulative distribution of the exponential distribution with empirical data from 102 measurements. We obtained the 102 data points by visually measuring the time it takes one ant to fill a slot and stay on top of another ant starting from when it becomes available. We performed experiments using central rods of 4 mm and 9.5 mm in diameter and measured 51 data points for each rod diameter. Visually, the fit is excellent. The Kolmogorov-Smirnov test value is confirmatory with confidence 0.95 (details are given on page 342-343 of Feller's book[60]). This gives some supporting evidence for the hypotheses. Based on the estimated value $\lambda = 65$ seconds and ant height $h = 3.0$ mm, the tower growth rate would be $h/\lambda = 2.8$ mm/minute if the ants were to stack up independently without building a ring. However, the predicted growth rate based only on these hypotheses is approximately three times too high to fit the data. Another factor must be coming into play.

We observe that narrow "fingers" of ants that grow upwards from the tower on the rod surface often peel and fall off the rod (see movie **S3**). In particular, the fingers that grow above an incomplete ring tend to peel off. We hypothesize that a ring is not stable until it is complete. A partial ring of ants would have to depend only on the adhesive force of a single ant to the central rod. We measure the adhesive force of a single ant to the

rod to be 2 ant body weight (2 dynes) which is equivalent to an adhesive pressure of 66 dyne/cm^2 acting on an ant area of 0.03 cm^2. To show that ants in a ring adhere to the rod more strongly than a single ant to the rod, we apply Laplace's law, $P = \frac{2T}{Dh}$ where P is pressure on the central rod, T is tensile force between ants, and D is the rod diameter. On rod diameters ranging from 4 mm to 19.5 mm, the adhesive pressure P ranges from 4500 dyne/cm^2 to 920 dyne/cm^2 which is 70 to 14 times stronger than the adhesive pressure of a single ant. Ants that build on rod diameters wider than 270 mm do not benefit from forming a ring. However, for the range of rod diameters in our study, the formation of a ring clearly increases the stability of the tower. Therefore, we introduce an additional hypothesis that is specific to the mechanics of towers: (4) the top layer of the tower is not stable unless there is a complete innermost ring of ants gripping each other around the rod.

Under hypothesis (4), the growth rate is governed by the time until the last space in a layer is filled. In Methods, we derive the following formula for the expected time for a new layer to form, based on maxima of independent exponential distributions,

$$E[T] = \sum_{k=0}^{k=S} \frac{\lambda}{S-(k-1)} \approx \lambda \log(S), \tag{2.13}$$

where S is the number of spaces in the ring. To test formula 2.13 of our ring-fill model, we ran a large set of trials on rod diameters ranging from 4 mm to 19.5 mm. Notice that it predicts different rates for different diameters D, since $S = \pi D/w$. The time to complete a ring, shown in **Fig.6D**, is a good fit with an R^2 of 0.66 until reaching rod diameter of 14 mm.

2.3.4 Sinking and rebuilding

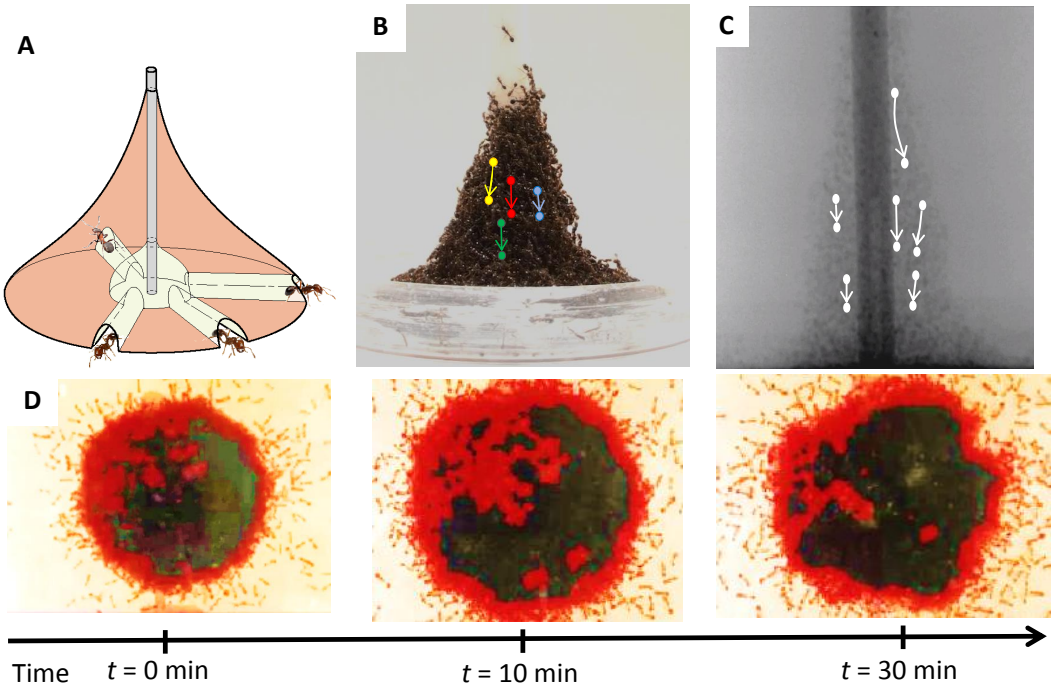

Figure 7: Flowing and rebuilding of ant towers. (A) Schematic of the tunnels observed underneath the ant tower. (B-C) Side views by video camera and x-ray showing ants sinking within the tower. The solid circles represent the characteristic trajectories of ants tracked over a period of 15 minutes. (D) View of the tower from below. The colors indicate the motion of the ants, black referring to no motion and red indicating the flow of traffic. The tunnels migrate, merge and disappear with time.

Ants on the surface (exterior) of the tower move rapidly in all directions atop the other ants. Ants below the tower surface appear to be immobile. However, time-lapse photography reveals that the ants in the tower's interior slowly move downwards. They tend to maintain their relative positions as the entire mass of ants sinks and exits through tunnels on the bottom as shown in **Fig.7A**. At high speed, the surface movements are a blur through which the sinking interior ants are visible. The sinking rate is approximately 0.38 $\pm$0.21 mm/minute based on 10 ant tracks from two towers (examples of 4 tracks are given in **Fig.7B**).

X-ray spectroscopy of fire ants that have ingested a radiographic contrast medium confirms the tower sinking (see movie **S4**). **Fig.7C** shows the downward trajectories of 6 ants. The iodine drink and X-ray tomography techniques were newly developed for this research, and may be useful in other studies of ant and other animal movement not visible to the eye. The details of the technique are described in the Methods section.

Where do the sinking ants go? The ant towers were placed in transparent petri dishes, which served as the base level of the tower. **Fig.7D** is a time sequence viewing from below the petri dishes. Evidently, ants are flowing downward. Ants build paths along the base surface, extending to the outskirts of the tower (see move **S5**). Ants enter the tunnels from inside the tower and exit, thereby joining the set of ants that move rapidly on the tower surface. Ants thus appear to clear a path in the tower similarly to removing soil underground. We note that ants do not remove other ants from inside the tower rather, they push other ants away in order to make a tunnel.

2.4 Discussion

Emergent structures have been studied for a variety of taxa including fish, ants, and bees[13,14,37,61]. In many of these early studies, a set of simple local rules for individual behavior are presented that lead to an observed group-level structure or behavior. In more recent studies, the rules of individual behavior are also validated by observation[62,63]. For example, Couzin et al. used rules of interactions between individual army ants and developed a model to explain their traffic flows[41]. The present study takes a step forward in that it identifies a consistent set of local rules, validated by observation, that lead to accurate predictions of the shapes and growth rates of both the ant raft and the ant tower[6,52].

The fire ant tower serves several important biological functions similar to the bivouacs[11]. It repels water, shields eggs in their interior, serves as a base of operations, and anchors the ants to land. Moreover, its construction uses decentralized control. The ants do not have to "know" that they are building a tower. All they are doing is moving randomly atop other

ants until they occupy an empty space adjacent to a stationary ant, just as they do when they build a raft. Unstable structures collapse, leading to a tower of constant strength as the only unique structure that remains over time. In the case of the tower, the only empty spaces are on the supporting rod immediately above the current top of the tower. Until all of the spaces at a particular height are filled, the structure is not stable enough to consistently support ants at a greater height. It takes a long enough time for all of these spaces to become occupied that this process is the bottleneck step, despite the geometric increase in the number of ants in an $n+1$ layer tower compared with an n-layer tower. Since the rod diameter is constant and the shape of the top part of the tower is invariant, this process increases the height at a constant rate.

In contrast, when the ants build a horizontal raft, all spaces at the perimeter of the raft are available to be filled, and there is no problem of mechanical instability. The building rate is not constant, and in fact tapers down to zero when the number of mobile ants is not sufficient to keep ants in the top raft layer stationary[6]. Essentially, the colony runs out of ants to expand the raft. From a dimensional analysis point of view, the colony never runs out of ants to build the tower upwards because a much smaller fraction of the ants are needed to keep the other ants stationary. The raft has constant thickness of about 2.5 ants. A completed raft of N ants therefore requires a number of moving ants proportional to N to keep the ants on the top raft layer stationary. A tower of N ants has surface area roughly proportional to $N^{\frac{2}{3}}$, and therefore requires a sub-linear number of moving ants. Hence the tower is circulant but the raft is not. Fire ants seem to be wasting energy to constantly rebuild the tower, so we speculate ants form tunnels, which causes the sinking, to alleviate high stress concentrations and to create pathways to transfer brood.

CHAPTER III

ANT AGGREGATIONS SELF-HEAL TO COMPENSATE FOR RINGLEMANN EFFECT

3.1 Introduction

Fire ants represent a new model system to investigate the self-healing of biological materials. They use their legs to link their bodies together in order to build both temporary and long-lasting devices, including rafts, bridges and bivouacs. These devices must be able to survive perturbations by the elements, including raindrops or rough water currents. How ant-built structures sense damage and repair themselves is poorly understood. In order for ants to self-heal, they must construct new structures of similar integrity to their old one, that is, one that is resistant to both compressive and tensile forces.

In this study, we show that fire ants compensate for Ringelmann's effect by self-healing. We first look into how ants connect and the strength of these connections. We developed experiments to show the strength contributions of connected and isolated ants inside a group. Lastly, we modeled the strength of ant aggregates as a function of time to heal their structures.

3.2 Methods

3.2.1 Ant husbandry

We procured ant colonies from roadsides near Atlanta, GA. Colony selection aims for an average ant weight of 1.5 mg. We removed colonies from the soil and placed into bins according to methods by Chen[53]. We fed ants baby food and pet food 3-4 times a week, along with constant replenishment of the water supply.

3.2.2 Micro-scale experiment

We measure the strength of leg-leg and leg-body connections to estimate the approximate load that the ants in an aggregate can carry while in the funnel with the cross-section area of 160 mm^2. We measure the strength of the leg-leg connection by tying an ant to the elastic band and another ant of the same colony to an inelastic string. We place the two ants in contact to stimulate a leg-leg connection. Once the ants attach their legs, we pulled the inelastic string which causes the elastic band to stretch at a fixed distance. We then equate this distance to a force using Hook's Law. We also measure the leg-body connection using the same technique while stimulating a leg-body connection.

3.2.3 Tensile test

We place 4.0 grams cluster on an analytical balance for all tensile tests and vary the top cluster. For the non-isolated tensile tests we put two ant aggregates in contact for contact times between 5 seconds to 15 minutes. For a group size of 1 ant, we tied 1 ant to a hair. For group size of 3-5 ants, we attach ants to a sponge. For group size of 30-100 we 3D printed funnels that has enough space for 30-100 ants to go through. For isolated tensile tests we tie each ant on a single strand of hair, each separated by 1 cm. We varied the group size between 1 to 4 ants. All set up are attached to a motor that can produce testing speed from 3.9 mm/s to 20 mm/s. The ant cluster on the bottom containing 4 grams is placed in a petri dish on top of a Metler Toledo analytical balance. We record the tests from the side view using Sony HDR-XR200 handycam.

For the 2D tensile tests, we put an ant pile of 5 grams on top of a petri dish lined with Velcro so that they will grip. We then place piece of Styrofoam of width 10 mm and depth of 3 mm. The force is measured by using a Futek LS200 load sensor at sampling frequency of 1 kHz and an Arduino Uno is used to measure the elongation length. All tests are performed at 10 mm/s.

3.3 Experimental Results

3.3.1 Qualitative observations of ants

Ants connect together using the hooks and sticky pads on the tips of their legs[49]. In our observations, we saw two types of connections occur, from leg to leg (**Fig.8A,B**) and leg to another ant's body (**Fig.8 C**). We conduct micro-scale experiments to measure the strength of leg-leg and leg-body connections. Leg-leg connections can support a tensile force of 195 $\pm$ 7 dynes; leg-body connection tensile forces are half as weak, at 69 $\pm$ 52 dynes.

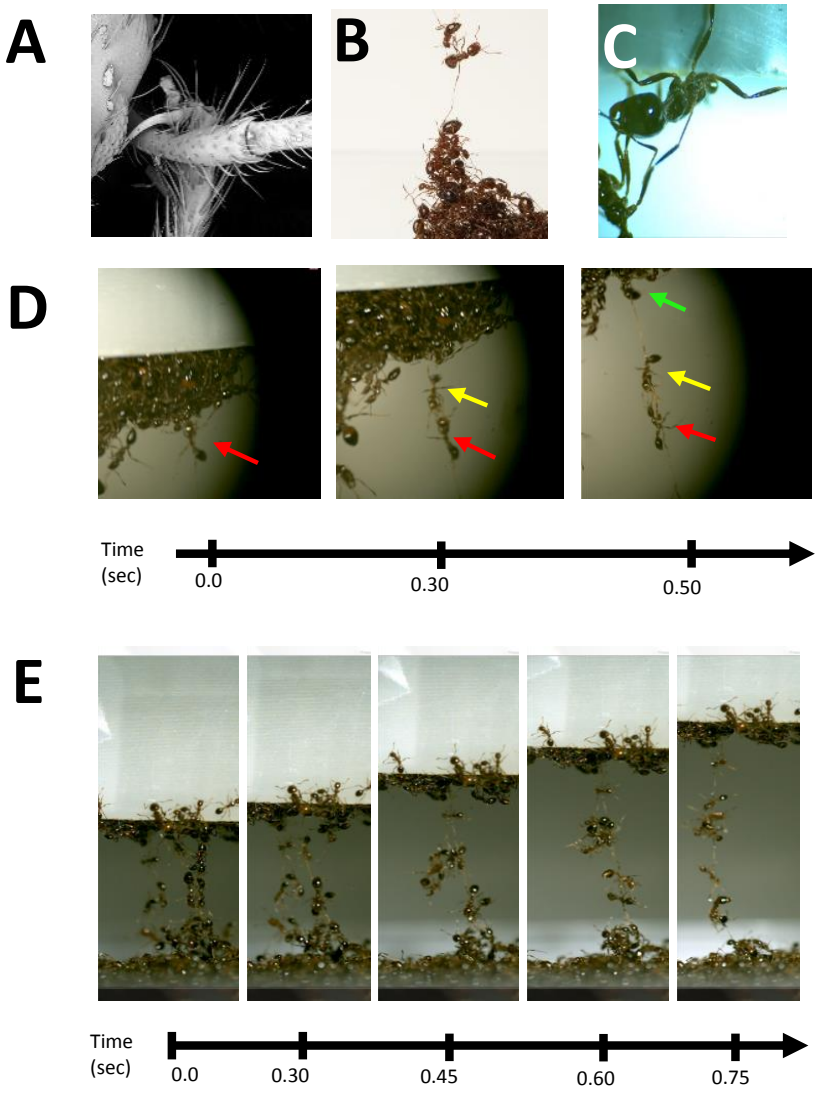

Figure 8: Cohesion of ants during tensile testing. (A) Close up of ants holding on to each other with tarsal claws. Photo credit - NJ Mlot (B) Ants holding onto each other using sticky pads on their legs. (C) A close up view of an ant string being separated from a cluster. (D) Ants linking together using leg-leg connections. (E) Two ant strings combining during a tensile test.

We took high speed videos of ant clusters being separated to visualize how they hold on to each other. Initially, ants form a mesh network that appears to consist of ants in random orientations. As the two clusters are separated, the network stretches out into multiple ‘’strings” of ants, oriented vertically and connected by their legs. **Fig.8D** shows

the formation of an ant string. As the clusters are separated further, the string appears to length as more ants are released from the cluster. Ant strings can also combine laterally to form longer strings. **Fig.8E** shows two separate strings of ants that combine to become a single string. We notice that as the structures are strained further, the connections slip, eventually becoming leg-leg connections, which are stronger than leg-body connections.

3.3.2 Ringelmann effect in ants

We conduct tensile tests with groups of ants ranging from one to one hundred. This range exceeds that of previous tests of Ringelmann's effect on humans. **Fig.9B** shows the different testing rigs fabricated to test this range of ants. The cross section of the testing rig indicates the number of ants tested, which are verified by counting ants during each test. **Fig.9D** shows the relation between contribution of each individual and number of individuals in a group. For comparison, we show data from human trials including tug-of-war, clapping, and shouting[64]. All data is normalized with respect to the contribution from one individual. Our ant experiments, highlighted in blue, shows that individual contribution per ant decreases dramatically with group size. Ants in a group size of 30 provide only 15 % of the tensile force of a single ant.

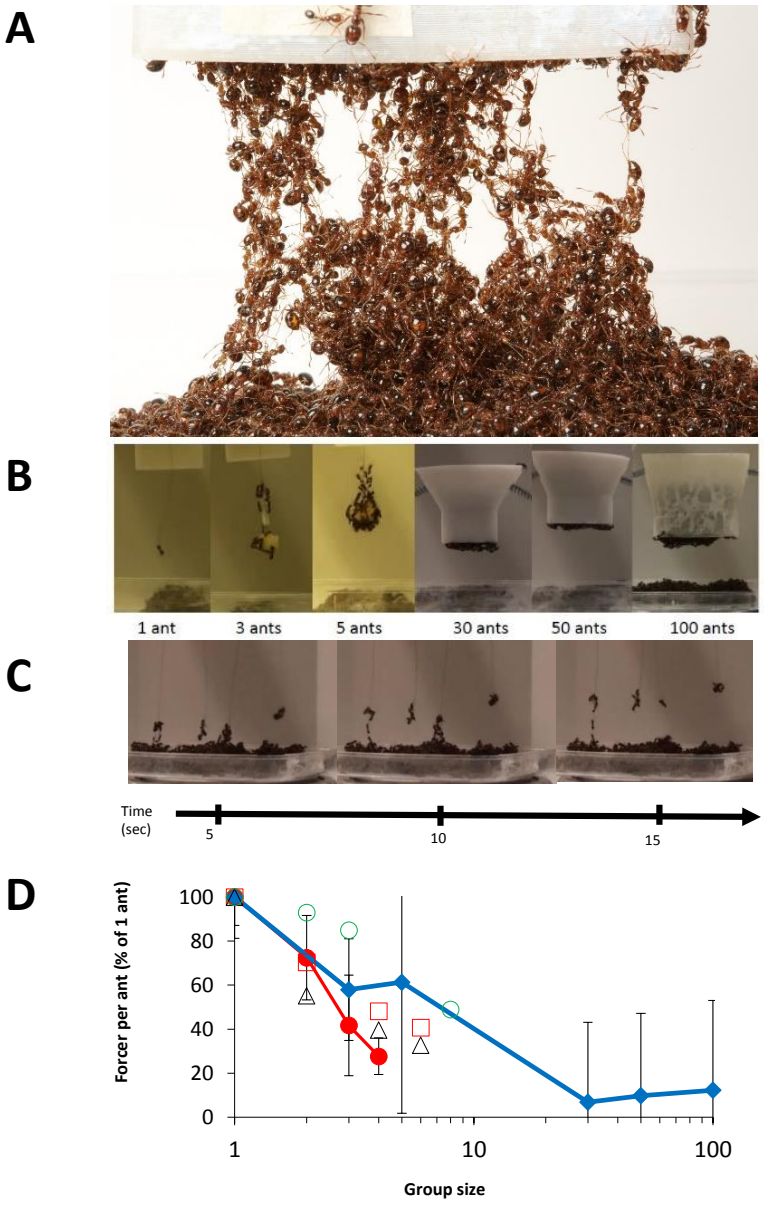

Figure 9: Tensile forces applied to ant aggregations. (A) Formation of strings and a mesh network due to separation of an ant aggregation pressed together for 3 minutes. Photo credit - Candler Hobbs. (B) Testing rigs to measure the strength of groups of ants (C) Four ants held apart by 1 cm undergoing ants a tensile test simulatenously (D) Relation between contribution per individual and number of individuals in a group. Green hollow circles correspond to tensile force in tug-of-war by Ringlemann, red hollow squares correspond to loudness of clapping, black hollow triangles correspond to loudness of shouting, blue curve corresponds to tensile force of group of ants in contact, and red curve corresponds tensile tests of group of ants not in contact, each separated by a distance of 1 cm. Contribution is normalized with respect to that of a single individual.

Ringelmann proposed that a lack of coordination was the cause of Ringelmann's effect. To test this hypothesis, we conduct tensile tests with ants isolated from each by individual testing rigs separated by 1 cm, as shown in **Fig.9C**. Here the ants can only communicate to each other through the force they feel through the string. In contrast, the previous test ants involved ants in direct contact with each other. **Fig.9D** shows the contribution per ant for both isolated ants (black line) and ants in a group (blue line). At a group size of 4, each ant is only outputting 27 % of individual strength which is less than the 65 % exerted by non-isolated ants for a group size of 5. The discrepancy suggests that the lateral connections made by ants might make the structures stronger. Nevertheless both tests show that Ringelmann's effect is a fundamental problem for ants. It is difficult for a group of ants to each exert their maximum force at the same time. This is partly because ants are different sizes and reach their maximum strain at different times. In the next section, we investigate how ants compensate for this problem.

3.3.3 Self-healing of ant aggregations

We press a pair of ant aggregations together for a given contact time τ_c, ranging from 5 seconds to 15 minutes. We then conduct a tensile test, pulling them apart at constant velocity. The state of an ant aggregation during a typical test is shown in **Fig.10B**. Such tests show an increasing tensile force, a peak in tensile force at T_{max} and then a decrease force as the aggregations begins to neck and fracture. The relation between force and strain during a test is shown in **Fig.10C**, where each color corresponds to a different contact time. Since it is difficult to measure the cross-sectional area, we define the tensile strength in units of force, dynes, rather than stress.

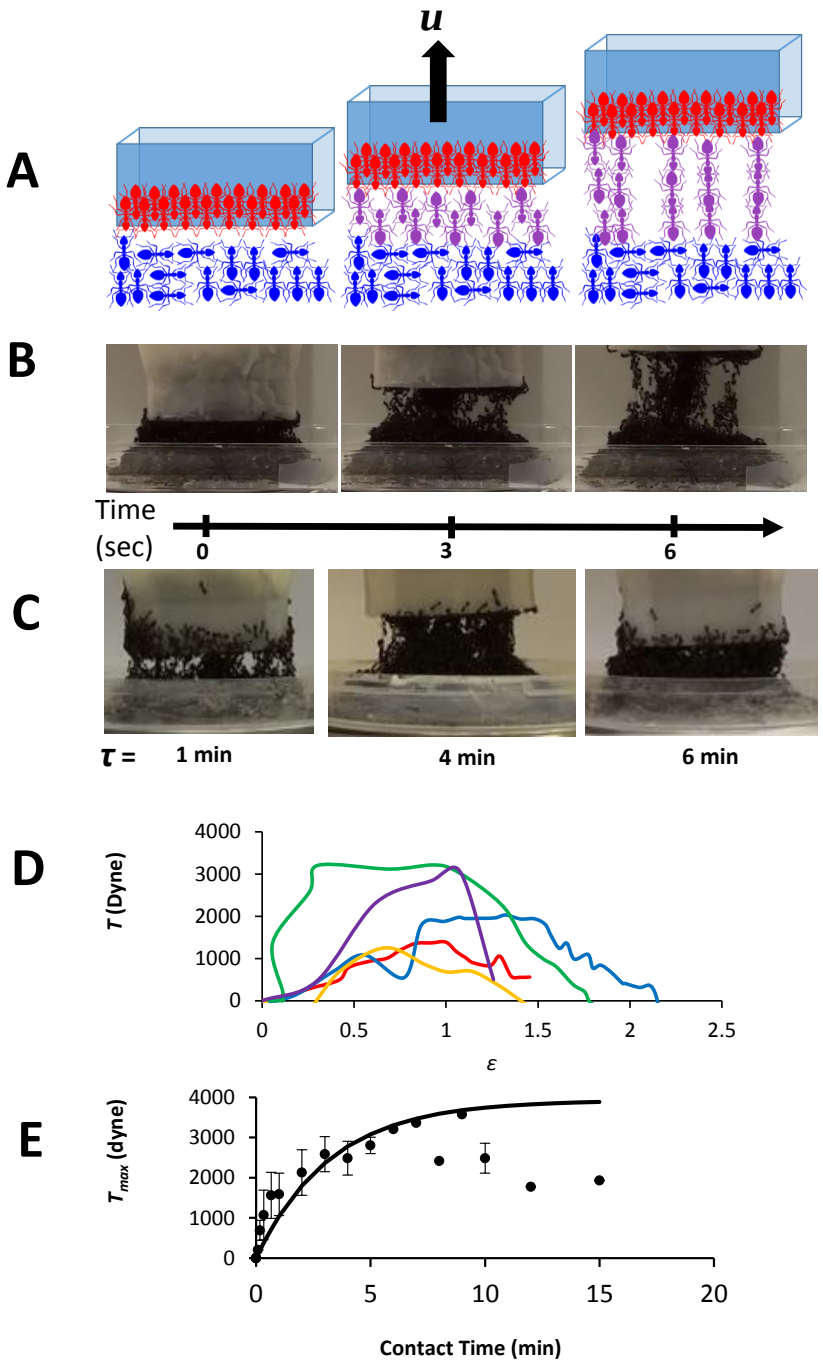

Figure 10: Tensile strength of ant aggregations. (A) A schematic showing the tensile test. Top cluster is red and bottom cluster is blue. The purple ants are the connections that form between the clusters. (B) Images of ants during a tensile test. (C) Images of ants during a tensile test at different contact times. (D) Force-strain plot of the tensile test for different contact times. The red curve denotes 2 minutes contact time, orange curve denotes 4 minutes, green denotes 6 minutes, blue curve denotes 8 minutes, and purple curve denotes 10 min. (E) The relation between tensile strength T_{max} and contact time.

Qualitatively, ants pressed together for longer times appear to show a greater number of ant strings, which correspond to a higher tensile strength. **Fig.10C** shows an increase in the number of ant strings with increasing contact time. We can measure this increasing strength quantitatively. **Fig.10E** shows the relation between tensile strength and contact time. The strength increases increases to a maximum of 3400 dyne at τ_c = 8 minutes. This amount is much less than the amount if each ant were to pull with maximum strength. Given the cross-section of the aggregation as 100 ants, we would expect a strength of 21,000 dynes if ants were attached with leg-leg connections, and 7,500 dyne if we assume all leg-body connections. Thus, ants are suffering a loss of strength per ant of 50% due to Ringelman's effect. We note the strength decreases to 30 % of the strength of τ_c= 8 minutes tensile test because ants have the natural tendency to explore and stop contributing to the in-lab structure.

3.3.4 Model of self-healing

We develop a model to explain this growth in strength, T, as a function of contact time, τ_c. Once the ant aggregations are in contact, ants move their legs randomly until they connect with a member of the opposite aggregation. Let $n(\tau_c)$ be the number of connections made between the aggregations, and N be the number of leg connections possible where N = two times the number of ants in a cross-section. The number of connections made per minute, $\frac{dn}{d\tau_c}$, is proportional to $N-n$, the number of appendages that have not yet connected:

$$\frac{dn}{d\tau_c} = \beta(N-n) \tag{3.1}$$

where β is a constant with units of 1/min. This differential equation explains the observations during experimentation. When we place two clusters in contact, initially there are no connections (n = 0). At first we find that the rate at which ants are connecting is very rapid. As n increases to approach N, the rate slowly plateaus. Solving the above differential equation yields the solution

$$n(\tau_c) = N(1 - \exp(-\beta\tau_c)) \tag{3.2}$$

where $n(\tau_c)$ is the number of connection as a function of contact time τ_c. Only connections that have been made can contribute to tensile strength of the aggregations. The associated tensile strength is found my multiplying by a constant α_s, which has units of $\frac{dynes}{connections}$ to get the theoretical ultimate strength value as a function of contact time

$$T_{max}(\tau_c) = \alpha_s N(1 - \exp(-\beta\tau_c)). \tag{3.3}$$

Thus, our model has two parameters, α_s and β that are found by curve-fitting, as well as an initial condition N given by the cross section of the ant aggregation. We use linear least squares to determine the tensile strength as a function of contact time. **Fig.10E** shows that the prediction of the model closely matches the trends. Our model also gives two fitting parameters of physical significance. We find each connection yields a force of α_s = 18.5 dynes. This value is 10 times less than than the leg-leg connection and 4 times less than leg-body connection measured from our experiment. We also find a rate constant by which self-healing occurs. The value β = 0.3 $\frac{connections}{(ant)(minute)}$ indicates that every minute, 1 connections are made for every 3 available connections. In another way, consider 3 ant appendages waving around randomly; one in 3 makes a connection every minute.

Our model can also predict how quickly the tensile force increases given the strain rate applied. In addition, we can predict the number of ant strings available for lifting ants as a function of contact time. We consider each of these strings pulling out ants from the aggregation at a rate of $u = 3.9\frac{mm}{s}$ or $\dot{\varepsilon} = \frac{u}{antlength} = 1.3\frac{ant}{s}$. Each of these ants lifted weighs m_{ant} where $m_{ant} = 0.0015$ g, gravity $g = 9,800\frac{mm}{s^2}$. Considering all $n(\tau_c)$ chains, the weight of all lifted ants per second is

$$\frac{dT}{dt} = \dot{\varepsilon} m_{ant} g n(\tau_c). \tag{3.4}$$

Fig.11A shows the time-rate of change of tensile force $\frac{dT}{dt}$ at $t = 0$, where the first 12 points for $t < 8min$ are considered. The model is given by the curve, which fits fairly against the data with a goodness of R^2 of 0.48. Note that there are no free parameters in this fitting; all parameters are found from the previous fitting of T_{max} and τ_c. Nevertheless, the fit suggests that the initial rate of increase in force is due to number of ant strings available.

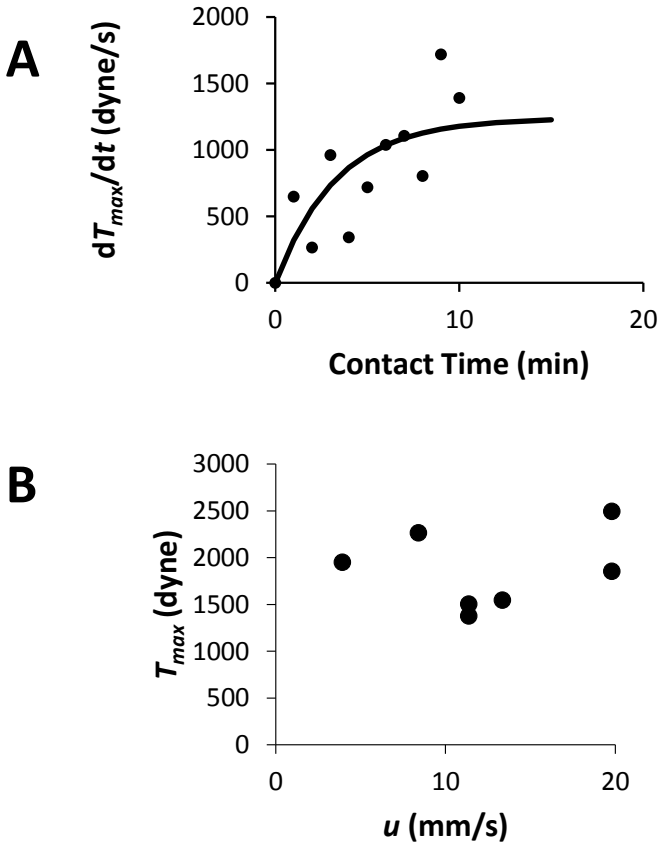

Figure 11: (A) Relation between initial rate of tensile force measured and contact time. (B) Relation between tensile strength and speed of tensile test.

Lastly, we show that the velocity chosen during our tensile tests does not strongly affect the outcome. We placed two clusters of ants for τ_c = 1 minute and separate the cluster at velocities ranging from 4mm/s to 20 mm/s. **Fig.11B** shows that the tensile strength falls between a small range of 14,000 to 25,000 dynes.

3.3.5 2D tensile test

We can compare the ant connections to entangled granular media. Staples are entangled granular media that show similarities to ant aggregates tested with extensional rheology. When a pile of entangled staples undergo an extension, the force vs. elongation curve shows many peaks that align with rearrangements of the staple pile. Tensile tests show that fire ant aggregates may experience rearrangement as seen by the peaks shown during the extension.

For the extensional rheology experiment, we perform an extension of a 2D chain of ants at a constant speed of 10 mm/s or $\sim$ 3 ant body lengths per second. **Fig.12A** shows a force vs. elongation of one of the tensile tests. Experimental procedures are explained in Methods. Due to the noise, we analysis the data using a 30-point running average. The force curve shows many peaks throughout the entire test which could be due to rearrangements of the ant connections. Unlike staples, ants are active and are able to move their legs around to make new connections to rearrange. However, the draw back is that they have joints. Their legs can bend and extend during the tensile tests which causes the ant aggregates to break when the limit is reach. As shown in **Fig.12B**, there is a general rise and fall throughout the elongation. This shows the ant aggregate reaching a peak force until a maximum point and the fall corresponding to the breaking of connections.

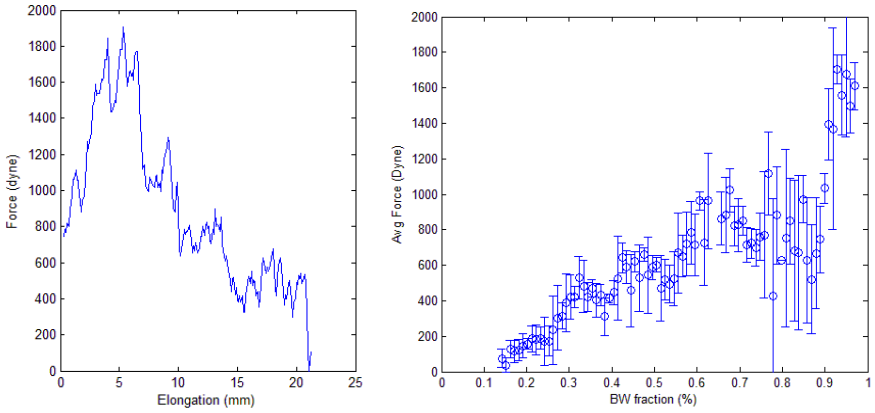

Figure 12: (A) Force vs. elongation curve of one of the 2D tensile tests. (B) Correlation between the density and force ($N = 3$) of 2D tensile test.

We can use image analysis to quantify the relationship between the density of the ant aggregates and the force. We equate the density to the fraction of the amount of space ants takes and total area they can occupy. Using least square regression, we find that there is a linear trend between density and force with an of R^2 of 0.67. From this, we may be able to visually predict the strength of an ant aggregation in 2D.

3.4 Discussion

This study showed that fire ants can self-heal their structures merely by being in contact with each other. However, it does take longer time to complete the repair as compared to growth of the ant raft. A cross section of 40 ants in our study took 8 minutes to reach equilibrium, whereas a sphere of 10,000 ants takes two minutes to reach equilibrium. Rafts initially grow faster as they become flatter, and ultimately have a very high growth rate at peak. as more and more ants become exposed. In self-healing, the rate is initially fast, but then decays because fewer ants remain available.

After a contact time τ_c of 8 minutes, the strength of the aggregate decreases. Thus, ants need further stimulation to remain in a group. This is also observed when a ball of ants are placed on a table. It eventually disperses. If we were to eliminate this dispersion from happening, we need to present a stimulant such as flooding or vibration that will cause the ants to cluster up. For 2D experiments, we can visually predict the strength of an ant aggregate. However, we cannot use the same method for 3D structures.

We still do not understand what leads to the rate constant β. Presumably, this constant reflects the rate that ants can find a place to grab in the opposing aggregation. This rate constant may be useful for simulations of ant connections under static and dynamic conditions.

CHAPTER IV

ENTANGLED ACTIVE MATTER: FROM CELLS TO ANTS

In this study of entangled active matter, we will focus on two model organisms, cells and ants. Since the advent of microscopy in recent years, there have been numerous examples of cells linking together to build larger structures[65]. For example, the slime mold, genus Dictyostelium, come together to build stalks to survive starvation. The cells in the stalk are rigid to increase the stability of the aggregate. Building these stalks increases the chance of being picked up by animals, washed away by rain water, and eventually transported to a location with a greater food source. In this paper, we will focus on murine sarcoma (S-180) cells, which are a common model cell used in cancer research because they can be easily injected in mice to test various cancer treatments[66]. These cells generally link to each other in clumps but can also metastasize, in order to colonize new locations. In this review, we report a number of methods that can be used to predict when cells metastasize, and how they will behave on different substrates. These methods treat the cells as soft matter, made active by virtue of the change of their properties in response to external cues.

The goal of this review is to develop clear analogies between cells and ants. We begin by enumerating the applications of studies of entangled active matter. We present methodology and results of mechanical tests that yield the bulk mechanical properties of cells and ants. Such tests are not possible with free active materials such as birds and fish. We then proceed to the dynamics of aggregates, going from the individual level of self-propulsion to bulk rates of spreading. We close with a few final thoughts and our perspective on the future of the field.

4.1 Results

4.2 Applications

The study of a single cell, or ant, is an entire field in itself, and much still remains to be understood how such complex organisms work. In our work, we have found often that groups of individuals seem to behave in ways that are simple to describe, but difficult to predict. Often, aggregations can form beautiful striking patterns. In part by the elegance of such patterns, studies of aggregates of these materials has found applications in a wide range of fields, including biology, medicine, agriculture, the food industry, and robotics. In this section, we discuss these applications.

Cellular aggregates are three-dimensional. Thus, they are good models for tissues and in vitro drug tests, because drugs active on a two-dimensional monolayer may be inefficient on three-dimensional tissue. Using cellular aggregates, prior to *in vivo* tests, saves the lives of millions of mice. Cellular aggregates can be formed by a number of ways, whose origins can be traced to other fields such as fluid mechanics or biology. One method, agitation uses a snowball effect to permit individual cells to attach to a ball of cells of increasing size. Another method, extrusion from a pipette such as in the pendant drop technique can generate a cellular aggregate whose size is based on the diameter of the pipette and adhesion of the cells. In Section 4.3, we will show how pendant drops can also yield mechanical properties of the aggregate.

Another way to create aggregates is to proliferate cells in confined geometries. This technique was started by J. Bibette for the perfume and food industries fields[67]. Later, P. Nassoy developed a microfluidic method of fabrication of elastic, hollow micro-capsules in which to grow cells. As the cells reach confluence, they swell the elastic capsule up to an 'homeostatic' state where the number of cell dividing is equal to the number of cells dying. From the deformation of the elastic capsule, one can estimate the homeostatic pressure[68]. Aggregates within capsules can be used to answer fundamental biological questions and

enable testing of novel therapeutic approaches. For example, the encapsulation of proliferating cells in an alginate (a polysaccharide extracted from brown algae) capsule is an important physical analogy. The work was first started in Institut Curie for cancer research because tumors in the body are generally composed of cancerous cells surrounded by a matrigel membrane. The rupture of this membrane may lead to a dissemination of the cells circulating in the vessels or migrating in the tissues. This strategy of confined tissue is now used to mimic stem cells generated from embryonic, adult, and induced pluripotent stem (iPS) cells.

Another great challenge is cellular therapy for the treatment of hair loss and skin reconstruction. For instance, the aggregation of adult human hair-follicle dermal papilla cells in 3D spheroids enables partial reprogramming sufficient to initiate hair follicle induction in recipient human tissue[69]. Recent findings by intracutaneous transplantation of bioengineered follicle aggregates indicate that it is possible to not only restore a hair follicle but also to reestablish successful connections with the recipient skin. This process can regenerate and sustain hair cycles[70]. Another important application of cell spheroids research is repair and eventually replacement of damaged organs by permitting stem cells to grow and restore the damaged areas inside the body. A recent example is the growth of a human ear on a mouse[71]. iPS cells are thought by many researchers to have a bright future to repair worn out tissues and to replace entire diseased or damaged body parts. Recently, a miniature brain-like organ, called the cerebral organoid, was made of stem cells aggregates and recapitulates some of the complex features of a growing brain[72]. Another application is the food industry: it is possible to grow a synthetic burger using stem cells from cows.

In this review, we primarily consider aggregates of murine sarcoma (S-180) cells transfected to express E-cadherins at their surface. S180 are fibroblasts taken from a mouse's epithelial sarcoma[73] that does not normally express cell adhesion molecules on its surface. We consider clones that are S180 cells stably transfected to express different levels of E-Cadherins. The transfection is made with the pCE-Ecad eukaryotic expression vector and

pAG60 as described in[74]. Generation of these cells and their observation require a microscope and often more sophisticated equipment. In contrast, ants are easier to visualize and to maintain in a lab. Thus, studies of ants can lead to more understanding of another way to generate collective behavior.

Studies of fire ants have application in agriculture and in robotics. Fire ants earned their name with the pain of their venomous sting. They are an invasive species to the United States, and are considered a pest. Fire ants cause losses of over one billion dollars annually due to the combined damage to crops, injury by fire ant stings, and destruction of property[75]. Fire ants are attracted to and aggregate in the electrical wiring of traffic signals, dying in such large numbers that they create clusters that short-circuit the wires[76].

The cooperation of ants has inspired much of modular robotics, the design and construction of robots that can link their bodies together and form larger more capable robots. Indeed, as technology advances, robots are built smaller and smaller, and more resembling ants in their abilities. In fact, discovering the principles of modular robotics was one of the Grand Challenges of Robotics in 2007[77]. Modular robotics has potential applications in exploration of challenging terrain. For example, a modular robot might separate itself into small pieces so it can more easily pass through the grate of a sewer. The robot could then reconstruct itself into a snake-like configuration to then clear the drain pipe[23–26]. Modular robots are also being considered for use extraterrestrial exploration where the price of payload transport requires robots to be brought up piecemeal.

Currently, modular robots have a number of limitations, making studies of fire ants useful to extend our understanding of active materials. First, modular robots can reliably connect to each other in relatively small numbers from 2 to 1,000 individuals[?], which is small compared to the several hundred thousands of ants that make up a colony[38]. Larger numbers of modular robotics are difficult to study because as the number of robot increases, so does the probability of encountering a non-operative robot. Thus, the manufacturing precision of modular robotics places a hard stop on their numbers. In contrast, because cells

and ants must adhere to each other actively, only live individuals remain in aggregations, while the dead ones fall away. Lastly, modular robots are also generally stiff and connect to each other in a cubic lattice. As we will see in the next section, cells and ants do not connect in a lattice, but do so randomly. This method represent an entirely new way to adhere together, and are providing an inspiration for building more dependable large-scale structures[78].

4.3 Mechanics

4.3.1 Scaling

The linkages between cells enable an aggregate to be treated as a single entity whose bulk material properties can be measured. The same is the case for ants, although because ants have a large amount of air spaces between them, bulk properties also depend on their packing fraction. Since the time and length scales vary, a number of different techniques are used to characterize cells and ants. In this section, we review their mechanical properties.

We begin with Table 1, which lists material properties of cell and ant aggregates. Since ant properties depend on density, we set the density of ants to be 0.34 g cm^{-3}, that of ants found at atmospheric pressure and room temperature[4]. The elastic modulus of an aggregate is measured using a rheometer or pipette. Surprisingly, cells and ants have nearly the same range of elastic modulus, with cells having 0.2 to 20 kPa[79], and ants 1-2 kPa. This finding may be related to the fact that other intensive variables, such as pressure, are also independent of body size[80]. This measurement does not include tendon and cartilage which can be much stiffer.

Table 1: A table showing some measurable properties of both cell and ant aggregates.

			Cells	Ants	References
Individual	Size	L	10-100 µm	2-4 mm	Purves et al. (2003), Tschinkel (2006)
	Mass	m	5 x10^{-13} g	1 mg	Godin et al. (2007), Tschinkel (2006)
	Walking speed	u	0.6-6 L/h	30x10^{5}-70x10^{5} L/h	DiMilla et al. (1991), Mlot et al. (2011)
Rates	Building Rates	r	35-50 h	3 min	Beaune et al (2014), Mlot et al. (2011)
	Time scale	$\tau_s = L/u$	1-16 h	2x10^{-7}-6x10^{-7} h	
Material Properties	Young's Modulus	E	0.2-20 kPa	1-2 kPa	Wells et al. (2008), Tennenbaum et al. (under review)
	Surface Tension	σ	1.6-20.1 dyne/cm	1000 dyne/cm	Foty et al. (1996), Mlot et al. (2011)
	Viscosity	μ	$10^8 - 10^9$ cP	10^6 cP	Forgacs (1998), Mlot (2011)
	Packing Fraction	φ	0.63	0.25-0.44	Martin (1997), Foster (2014)
Adhesion Force (Nondimensionalized by body weight)	Agents		50x10^{-12} N (0.1 N/mg)	3 x10^{-3} N (0.003 N/mg)	Puech (2006)
	Substrates		30x10^{-12} N (0.06 N/mg)	10^{-5}-3x10^{-3} N (0.00001-.003 N/mg)	Pelham (1997), Dejean (2010)

There is no agreed-upon method to measurement for ant surface tension, so we consider $\tau = EL^{-1}$ where E is the Young's modulus and L is the length scale of an ant. Using this method, we the surface tension of ants is in the range of 10^3 dyne cm^{-1}, while the surface tension of soft tissue is much smaller, at 1.6 - 20.1 dyne cm^{-1} [6,81]. Thus, the surface tension of ants seems to be 10 times larger than water and even slightly larger than mercury. We find the high surface tension of ants to be surprising, but the surface tension is consistent with the large size of ant balls that we can make by hand, about 2 cm in diameter, suggesting a much large capillary length compared to that of water, which has a capillary length of 2.3 mm.

The viscosity of these aggregates indicates how easily they flow and dissipate energy. Because both cells and ants flow very slowly, their viscosities are both very large. The viscosity is 10^8-10^9 cP for cells as compared to 10^6 cP for ants[6,82]. The higher viscosity of cell aggregates can be attributed to their higher packing fraction of 0.64 (quite similar to a random close packing of balls) as compared to ants of 0.2-0.4[49,83]. Elastic modulus,

surface tension and the fundamental variables used in the mechanics in this section. In the next section, we discuss how mechanics can be used to infer forces from these variables.

4.3.2 Physical picture

Since the pioneering work of Malcolm Steinberg who was the first to claim that tissues are liquids[84], the mechanical properties of cellular tissues are still debated. Analogies with soft matter bring valuable insights into the rheological properties of tissues. At first sight, cell packing in a tissue is very similar to the packing of bubbles in foams. If this analogy has been fruitful to describe the statics properties of cell configuration in tissue development, it does not hold for the dynamics of tissues. Foams are solid, and flow only above a yield stress σ_y. Tissues, on the other hand, are ultra-viscous liquids similar to polymer melt: below a tissue relaxation time τ ($\sim$ few hours) they behave like a rubber with an elastic modulus E. Above τ, they flow like a liquid, with a viscosity $\eta = E\tau$. This is a common feature for both cells and ants: cell aggregates and ants swarms squeezed between two plates behave as a rubber and quickly round up again after compression (**Fig.13**). These aggregates are also named spheroids because, as liquid droplets, they minimize their surface energy adopting a spherical shape. Given time, these same aggregates will spread like liquid drops.

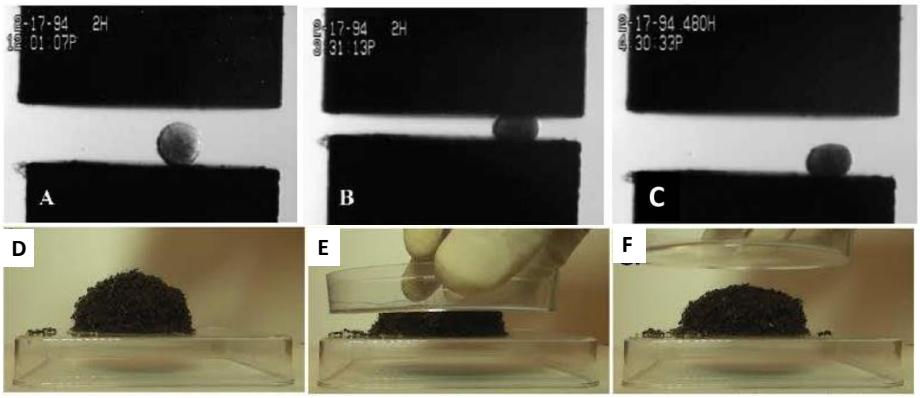

Figure 13: (A-C) Cell aggregates (top) are elastic at short time and behave like a rubber. At long time $t > 1$h, they flow like a liquid. Photos adapted from[2] (D-F) Ants swarm (bottom) also behave like Silly Putty paste for short times. Photos courtesy of Michael Tennenbaum and David L. Hu.

The difference between foams and tissues is due to the noise produced by the living cells. Thermal agitation is not strong enough to reorganize the structure of foams to relax mechanical stresses. The energy barriers corresponding to the reorganization are much larger then thermal agitation energy and the system is frozen. On the other hand, cells are active and produce a large noise, which explains why tissue can flow. Similarly, aggregations of ants also produce large noise and behave in a similar way.

Back in the sixties, Malcolm Steinberg was the first to find this unexpected behavior and to measure the surface tension γ of organs[?] . Mixing cells of two tissues, he observed cell sorting. And, as liquid droplets, tissue with lower surface tension engulfs the tissue with higher surface tension γ[2]. Steinberg's hypothesis that cell sorting in tissues arises from differences in surface tension between different cell populations has gathered extensive experimented support[85]. The most widely used technique to characterize tissue properties has been parallel-plate compression introduced by Steinberg and co-workers[82]. Compressed

between two plates, aggregates behave as viscoelastic droplets. From the measurement of the time course of force, one can derive the elastic modulus at short times and the surface tension at long times[86], but this technique is difficult to use and cannot be applied in vivo.

We have developed a novel method based on aspiration by micropipette to investigate tissue mechanical properties[87]. The aggregate is aspirated at a constant suction pressure into a micropipette (**Fig.14**), at a pressure $\triangle P$ larger than $\triangle P_c = 2\gamma(R_p^{-1} - R^{-1})$ where R_p and R are the micropipette and aggregate radii, respectively. We use this technique to measure the viscosity η and observe cell activities due to change in $\triangle P$.

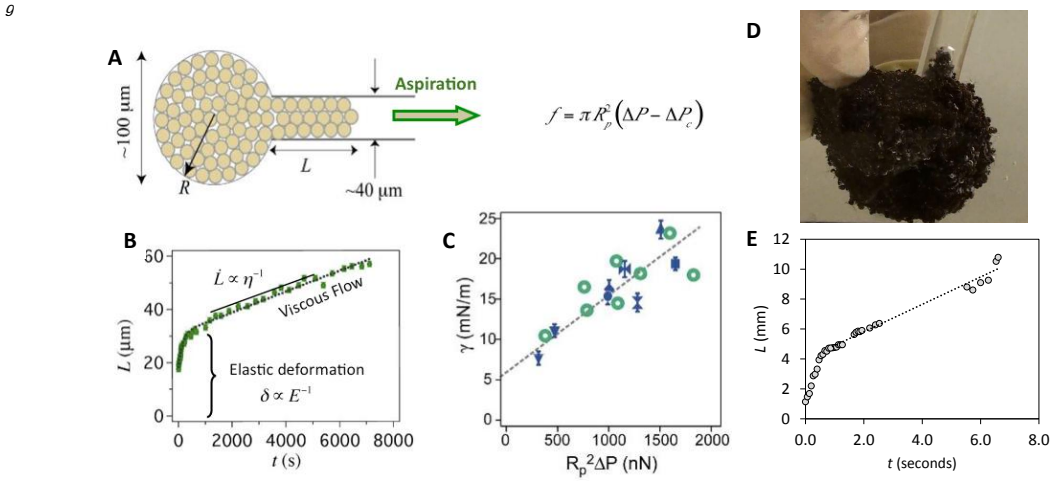

Figure 14: Aggregate aspiration. (A) Illustration of micropipette aspiration of spherical cellular aggregate. $\triangle P_c = 2(1/R_p - 1/R)$ is the threshold aspiration pressure. (B) Aspiration cycle for an aggregate $\triangle P = 1180$ Pa, with $R_0 = 175$ microns, and $R_p = 35$ microns (C) Surface tension η (mN) as function of applied force $R_p^2 \triangle P$. Adapted from[3] (D) Image of the aspiration of a spherical ant aggregate. (E) Aspiration cycle of an ant aggregate.

First, the surface tension γ increases with $\triangle P$ (**Fig.14 C**), showing that cells stretched in the capillary react by reinforcement of the cortex, which is a layer of the cytoplasm that supports the plasma membrane. Second, in a narrow range of pressure $\triangle P$, we observe pulsed contraction or a 'shivering' of the aggregate: a signature of the molecular motor

activity induced by external forces. It has also been observed that forces exerted between cells in a developing tissue under stress are not always monotonically varying, but can also be pulsatile[88]. Although arising from different kinds of forces, that behavior is reminiscent of the intermittency observed in certain flow regimes of dry granular matter when moving through an hourglass-type constriction (called 'tickling effect')[89], and also the intermittent motion of ants trying to escape through a constriction.

Our measurement of mechanical properties using pipette aspiration is now widely used. All in all, the main conclusion is that aggregates behave like 'living' viscoelastic liquids: they reinforce their mechanical properties with pressure, showing a mechano-sensitive active response of the acto-myosin cortex. Acto-myosin cortex is a layer of protein on the cell membrane that controls the cell shape. The aspiration method can also be used for ants held underwater. The results show similar regimes: an elastic regime and viscous regime as seen in **Fig.14** from which we can extract the viscosity. In the experiment showed in **Fig.14D-E**, the viscosity was found to be 4.3e5 cP which is close to the value found by Mlot *et al.*[6]. However, we will show that ants are shear thinning so their viscosity changes with applied stress.

The mechanical properties of ants was measured in an experimental study by Tennenbaum et al.[4]. The rheometer setup is shown in **Fig.15A-B**, where velcro is used to ensure no-slip. In a variety of conditions, ants were shown to be able to both store and dissipate energy. Controlled shear rate experiments were performed in which we measured the stress required to maintain a constant shear rate. Aggregations of 3000 ants were used. For a wide range of strain rates (10^{-2} to 10^{1} s^{-1}), there is a plateau of stress. This stress shows that ants are indeed resisting the rotation of the rheometer. Moreover, this plateau is reminiscent of the plateau of polymer melts[90,91], which maybe indicate that the stress is due to the disentanglement of the connections of both ants and polymer melts. The ants flow according to the constitutive relation for ant viscosity, $\sigma = \eta\dot{\gamma}$, where σ is the stress, $\dot{\gamma}$ is strain rate. The viscosity η decreases with strain rate according to $\eta = \sigma_0\dot{\gamma}^{-1}$. The constant σ_0

of 70 Pa is consistent with a dissipation due to the high friction within the joints of ants, which friction coefficient is three orders of magnitude higher than for human joints[92,93]. Both live and dead ants satisfy the same constitutive relation, indicating that live ants 'play dead' when forced to flow.

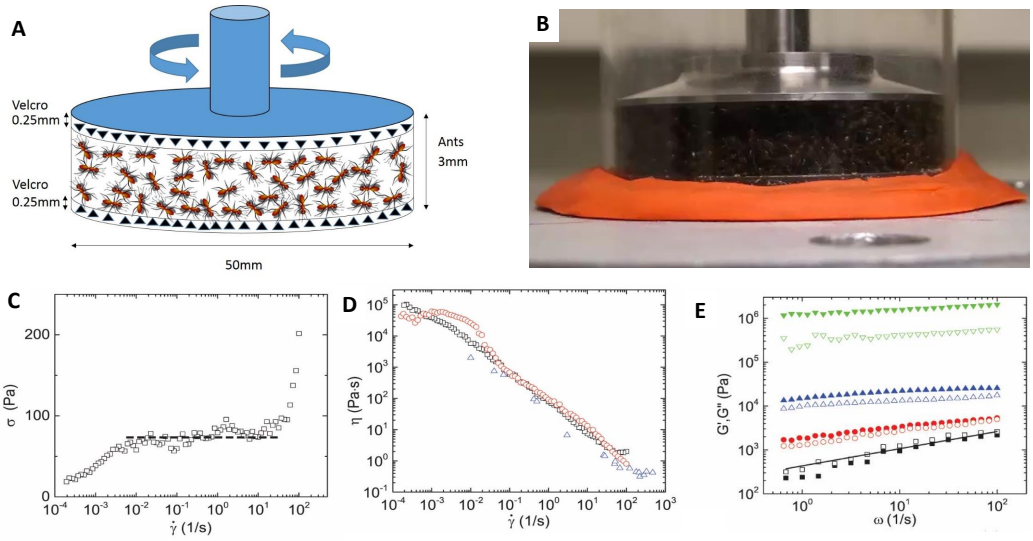

Figure 15: (A) Schematic of ants inside the rheometer set up. Velcro is attached on the top and bottom walls to create a no slip boundary. (B) Image of the rheometer set up. (C) Shear stress, σ, as a function of applied shear rate, $\dot{\gamma}$. For a large range of shear rate, 10^{-2} to 10^{2} s^{-1}, the stress remains at a constant 70 Pa. (D) Viscosity, η, as a function of shear rate. The squares are the viscosities that result by dividing the stress and the shear rate shown in a. The circles correspond to a similar experiment where the shear rate is progressively increased from 2 x 10-4 s^{-1}. The triangles correspond to viscosities taken from creep experiments where a stress is applied and the strain is measured as a function of time. The black star is the viscosity from the falling sphere experiment from which we extract a shear rate, which we can convert into a viscosity by using the value of the applied stress. The ant density in all these experiments is 0.34 g cm^{-3}. (E) Frequency sweep in the linear regime for live ants at a density of (squares) 0.34 g cm^{-3}, (circles) 0.68 g cm^{-3}, (triangles) 1.02 g cm^{-3}, and (upside-down triangles) 1.36 g cm^{-3}. G' (closed) and G" (open) are shown. As the ant density is increased the congruence observed for ρ = 0.34g/cm3 disappears and G' progressively becomes larger than G" and becomes more frequency independent. Photos and chart adapted from[4]

We also perform creep tests in which we apply a constant stress and measure the strain

rate, as shown in **Fig.15C**. This test describes how willing the ants are to release each other under duress. We find that ants do not behave like a simple fluid. For applied stresses between 40 and 70 Pa, we observe periods where strain is linear with time and others where strain is constant. The ability of ants to hold themselves stationary indicates that they are able for brief periods to store elastic energy. For applied stresses above 250 Pa, ants are torn apart, indicating that the stress which they resist during flow is only 4 times less than their maximum.

We also perform oscillatory tests in the linear regime to greater understand the ability of ants to store and dissipate energy. **Fig.15D** shows the strain rate dependency of the viscosity. In addition, **Fig.15E** shows the elastic modulus G' (closed circle) and storage modulus G" (open circle) as a function of frequency. As ant density increases, there is a clear separation between G' and G". Moreover, as density increases, the two moduli become frequency independent. For low densities, ants behave like a critical gel, in which G' and G" are equal. For high densities, live ants are primarily elastic and have a similar G' to dead ants.

The mechanics of entanglement shares some similarities with linkages of u-shaped particles. Gravish et al. find that the entanglement due to the bent ends of *u*-particles increases the stability of the pile[50]. Franklin shows how entanglement of *u*-shaped particles can resist extension. During extension, there is a stick-slip inside the pile in which weak links break but the links rearrange, maintaining a cohesive pile[?] . There is also a similar behavior when ant aggregates undergo constant extension. More work must be done to understand how ant aggregations exhibit this range of mechanical behaviors.

4.4 Dynamics

Analogies between living tissue mechanics and dynamical phenomena involving liquid interfaces known as wetting phenomena have been used to explain several ubiquitous tissue

behaviors. A striking analogy between tissue mechanics and liquid wetting is found in tissue spreading. For instance, when two aggregates of cells or ants are brought into contact, they coalesce to form a single larger spheroid[88]. One can see the spreading and the fusion of two aggregates of cells and ants of radius R in **Fig.16**. From γ and η measured with the pipette aspiration for cells[87] and γ and η measured by Mlot *et al.*for ants[6], we can define the capillary velocity $V^*= \gamma\eta^{-1}$ ($\sim 10^{-8}$ ms^{-1} for cells and $\sim 10^{-3}$ ms^{-1} for ants). A scaling relationship ($V * t = R$) leads to spreading times t of order 6 hours for cells and 3 minutes for ants. We also show in **Fig.17A-B** a striking analogy between the spreading of ball of cells and ants.

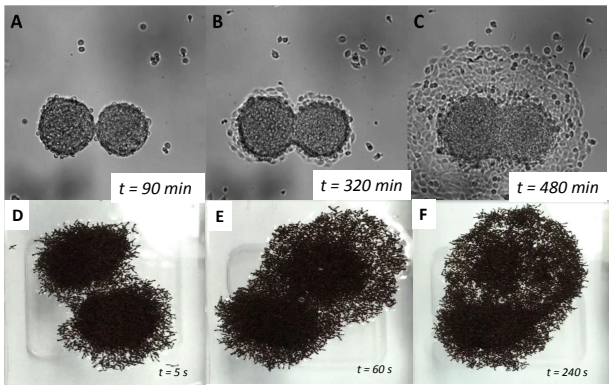

Figure 16: (A) Fusion of cellular aggregates. (A) Two aggregates in contact, courtesy S. Douezan. (B) A neck connects the aggregates and (C) Spreading and fusion of the aggregates. Scale bar corresponding to 100 microns. Photos courtesy Stéphane Douezan. (D-E) Two ant rafts come into contact, fuse, and spread.

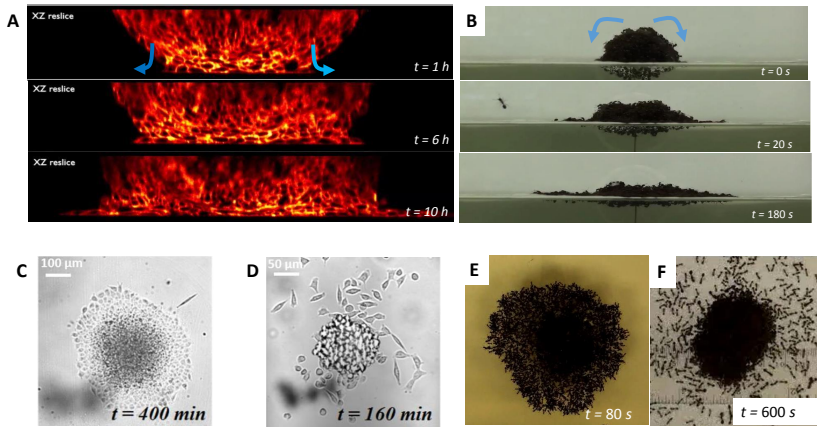

Figure 17: The spreading of cell and ant aggregate from a ball to a pancake shape. (A) An image sequence of ball of S-180 cell spreading on a substrate over a period of 10 hours[5] (B) An image sequence of 3,000 ants spreading on top of water over a period of 3 minutes. Free ants on the surface walk and attach to the edge of the raft, thus growing it[6].(C-D) Cell Aggregate Spreading: Liquid and Gas phase of the precursor film, from left to right[3]. (E-F) Top view of the spreading of ants on water which shows the cohesiveness vs. land which shows a looseness of the aggregates.

When a cell aggregate is put into contact with the substrate, we find two regimes of spreading. At short times, the aggregate flattens. The spreading area follows a universal law interpreted in analogy with the spreading of a viscoelastic droplet[3]. At long times, a precursor film made of one cell monolayer spread around the aggregate. We interpret the dynamics of the precursor film from a balance between the gain of surface energy, and the viscous losses associated with the permeation of cells from the 3D aggregate into the 2D film[5,94]. The slippage of the surrounding monolayer is negligible. On patterned substrates with adhesive strips separated by non-adhesive PLL-PEG bands, we observe a spreading of the monolayer on the stripe at constant velocity V^* ($V^* \approx 7.9\ 10^{-9}$ ms^{-1} on glass coated with fibronectin), demonstrating that permeation is the factor limiting the spreading[94].

We have studied the spreading of balls of cells that express a tunable level of cadherins. These balls are placed on various substrates, such as glass substrates and polyacrylamide gels decorated with extracellular matrix (ECM) protein fibronectin. In particular,

the physics of wetting had been applied to describe the tissue's wetting transitions in term of a single spreading parameter S, which for liquids measures the difference between cell-cell affinity and cell adhesion to the substrate. If S is negative, corresponding to large cell-cell adhesion (controlled by a high level of cadherin expression), the living drops do not spread. This regime is called 'Partial Wetting'. If S is positive, corresponding to a strong adhesion with the substrate, the wetting is complete, with a precursor film (a cell monolayer) escaping from the drop. A wetting transition can be induced by using tunable adhesive substrate (PEG-Fibronectin surface treatment or substrate rigidity). In complete wetting, we observed two states of the precursor film. If the strong cell-cell adhesion, the precursor film is in a cohesive liquid state. For weak cell-cell adhesion, the film is in a gas state, and so cells escape from the aggregate individually. This liquid 'gas transition' corresponds to the epiyhelial-mesenchymal transition introduced in biology for cancer metastasis and processes in embryonic development. Remarkably, this behavior is also observed with ants. When ants spread on water, they form a very cohesive film. On land, they do not stay connected but begin to escape from the aggregate in a gas state. Therefore, they spread in manners similar to cells, as shown in **Fig.17C-F**.

The gas state of these individuals can also be referred to as the 'dilute limit.' Much of ant activity is performed in this dilute limit, especially for species that do not form aggregates. For example, foraging activity may occur either by individual random walks (or perhaps Levy flights), or by means of well-organized foraging trails where ants move most of the time without touching each other with the exception of short inter-antennal contacts[95–97]. Even in experiments where leaf-cutting ants are constrained into a 2-dimensional Hele-Shaw cell and excited by an insect repellent fluid, the individuals try to avoid 'entanglement' among them, and behave even 'politely' if they need to escape through a narrow door, as illustrated in **Fig.18A-B** : this behavior, different from the common attitude of humans in panic, prevents jamming at the door.

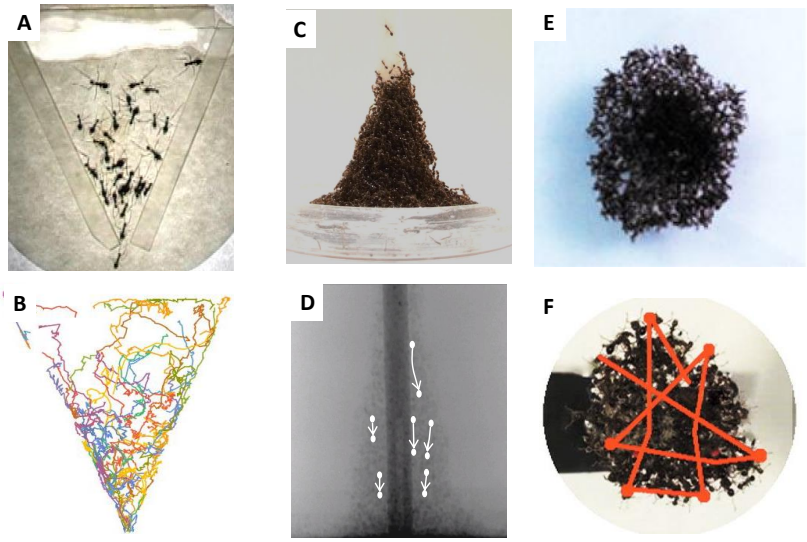

Figure 18: Ant motion. (A). A snapshot from a video taken to ants from the species Atta insularis into a triangular, two-dimensional Hele-Shaw cell. Ants try to escape but never jam or connect during the escape. (B). The colored lines in the picture are ant trajectories associated to the whole video, which reveal that loops and intermittent motion are typical of escaping ants in a 'panic' situation (Picture courtesy of J. Fernndez, F Tejera and A. Reyes). (C). A snapshot of the side view of an ant tower. (D). X-ray of the ant tower shows that ants inside the tower also sink over time[7]. (E). A snap shot of the top view of an ant raft spreading over water. (F). Tracks of ants moving on top of a raft over the duration of the spreading. Photos courtesy of Nathan Mlot & David L. Hu.

In another experiment, a Hele-Shaw cell with two symmetrical exits is filled with leaf-cutting ants[98]. The ants are excited by a repellent fluid in the middle, ants tend to follow each other. The resulting crowd eventually breaks the symmetry by using preferentially one of the two doors. While that phenomenon increases the total escape time from the cell, it does not mean that ants jam at the selected door, endangering their lives: they try to avoid entanglement, and even retreat from the door if other ants are already trying to get out at the same time. Then, ant-ant entanglement occurs only in the 'high density limit' of certain species of ants, in order to perform specific tasks, which results in a unique soft matter phase on which this review is basically focusing. From the experimental point of view, it is worth mentioning that, even in the 'dilute limit', tracking of ants based on videos is a

difficult task as soon as bodies touch each other.

There remains much work to be done to understand how cells and ants sense and respond to their environments. We know cells are sensitive to the surrounding environment; they feel the rigidity and the forces applied on them. Our living drops can therefore be described as 'active' viscoelastic pastes, able to react to the forces applied on them by a reinforcement of their mechanical properties. Ants are also sensitive to their environments. On land, they don't stay in a cohesive cluster but spread out individually. On water, they stay connected while they spread. Only in this bulk state can we obtain measurable properties to compare to cell aggregates.

4.5 Conclusion

Cells and some ant species show remarkable resemblances in their collective behaviors that call for interdisciplinary studies to strengthen the analogies between the two organisms. We showed that even though cells and ants communicate and self-propel in very different manners, there are some common underlying behaviors. They have means to connect to each other and to substrates, communicate with each other, and navigate their environment. In addition to these basic features, the rules that governs both of these organisms results in complex motions that arise through interactions with their peers. We also showed that when in an entangled state, we can study and characterize the two systems. Although they interact in different scales and have large differences in their physical properties, there is still a need to find common test methods to characterize other properties of these two organisms. These studies could influence the field of collective motion, active matter, and soft matter.

One of the big challenges in the study of ants and cells is their opacity. We still do not have an easy way to see inside the structures. How ants move inside an aggregate has yet to be systematically studied. Ants are accustomed to moving in small spaces, such as within tunnels. Their legs, which are fully extended as they walk on flat substrates, are

also capable of propelling the ants within small tunnels. As the packing fraction of ants is increased, the inherent motion decreases. We call for the need of methods to effectively track ants inside their structures in real time. Certain ant species build 3D structures such as bridges and bivouacs whose internal structures are not easy to visualize. Methods such as the one used by Foster et al. are useful for looking into snapshots in time of ant structures[49] but better methods of data collection are needed to study the construction, maintenance, and disassembly of these structures in real time. One possibility is using x-ray to track the activity of ants inside their nest, that is otherwise obstructed from view[99]. Similarly, new methods such as dynes replaced by two photons microscopy are being developed for visualization of cells within aggregates[5].

It remains difficult to track the individual motion of large groups of ants, but there have been some progress in the last years. Vision based tracking of multiple objects has improved over several years and can be useful in applications where ants are set up in a 2D environment[100,101]. However, it is still difficult to track the activity in ants at the colony level. Noda et al. developed a device that can track long terms activity of ants the coming and going into their nest with great accuracy, and during extended periods of time[102]. This device could prove useful in tracking the activity of the colony in wild conditions. More recently, however, ant tracking has reached a qualitatively new level by implanting tiny 'radio tags' on individual ants, which has allowed, for example, to understand the collective decision-making process in ants[103].

Both cells and ants have much to reveal about the study of active matter. Moreover, concepts of soft matter and wetting have been very fruitful in unveiling striking analogies between the physics of inert soft matter (polymer, viscous pastes, silly putty) and the behavior of biological tissues and swarms of ants The comparative study of these cells and ants aggregate could lead to new experimental methods and modeling techniques that may have applications from tissue engineering to robotics.

CHAPTER V

CONCLUDING REMARKS

In this study, we show that fire ants build towers of particular shape. This shape allows each ant inside the tower to hold equal amount of weight, 2.6 ants. In addition, we modeled the rate at which they build these towers using only one experimentally measured value, the time for an ant to occupy a space. From the outside, the towers looks static once it's finished growing, however, a high speed video of the tower reveals that it is constantly sinking. We further show this by performing an x-ray experiment on the tower during after it reaches equilibrium state and validated the sinking behavior. As of now, we do not have a clear answer as the why the tower sinks after it's finish building. However, we speculate that the tower sinks due to the tunnels that ants excavate underneath the tower. Visually, the tunnels seems to be a pathway for ants to circulate from inside to the outside to continue maintaining the tower. It also appears to be a means for ants to move broods and eggs inside the tower for protection. There needs to be more experiments to fully answer this question. A way to find if ants harbor broods and eggs underneath the tower is to leave eggs/broods outside after the tower has been built and track the movements of those eggs/broods. One way to find a reason for the sinking would be to map out the stress underneath the tower. Ants may intentionally create tunnels to relieve stress that are too high for broods/eggs because we know that fire ants can hold stress much greater than 2.6 ants.

We measure strength of fire ant aggregates in varying sizes and showed they self-heal short durations, but then separate over long durations. Tensile testing allow us to measure the strength of the aggregates as a function of group size and contact time. This study shows that each ant contributes less to the group as group size increases. When two clusters are joined together, fire ants will self-heal into one connected structure. Using modeling, we

found that the rate of connections made is proportional to the number connections not yet connected. The rate at which new connections form decreases until saturation. In addition, the 2D tests show that there is a correlation between the number of connection and the strength of the aggregate. Higher densities results in higher forces measurements. There are still some questions left to answer. We might be able to find a physical analogy or simulation to verify the connections made by the ants to show that they have a stick-slip behavior when they undergo extension. We are able to model the strength of self-healing ant aggregations as a function of contact time under no stress conditions. However, for it to be a more biological relevant model, we need to vary outside conditions which could lead to different parameters other than contact time. In the wild, ants are exposed to instant changes in conditions such as heat and disturbances from wind and water.

We compare the collective behavior of cells between ants and show some similarities in their bulk properties. Although these two organisms work in different scales in terms of sizes and time, we show that some common experiments of the two can be used to extract their physical properties such as the aspiration technique. For short times, these two aggregations behave like a solid but over long time scale, they behave like a liquid. There may be some rules that govern the behaviors of these two organisms that may reveal ways to study entangled active matters even though the mechanism that they communicate and connect are vastly different. However, one of the biggest challenge against studying these aggregations is developing methods to visualize the internal interactions between the individuals. If this is possible, we may be able to develop models and experiments that connects the micro scale interactions with the macro scale behaviors of similar active matters.

The study of collective motion of ants can have implications in many fields including active matter, self-healing materials, and robotics. Even with simple rules, ants can accomplish many complex tasks in their harsh environments and thrive. Much can be learned from the physical tools that they posses in the design of swarm robots such as the way they

communicate and connect to each other. In addition, these ants have potential to be a good model to the study of active matter and self-healing material. They are easy to visualize and are readily available. If we can build a good comparison between ant aggregations and other organisms, we may be able to develop new methods that review the inner workings of entangled active matters.

APPENDIX A

SUPPLEMENTARY VIDEO CAPTIONS

Video S1. Time lapse video of ant tower construction around rods of diameter 6.4 mm and 11.2 mm. Video is sped up 128 times. **https** : //**youtu**.**be**/**Cc7w2odIXSA**

Video S2. Close up view of ant tower construction on an 8 mm central rod. Video is in real time. **https** : //**youtu**.**be**/**tK609ZnCBwQ**

Video S3. A finger of ants peels off the central rod, indicating the importance of ring formation in making stable towers. Rod diameter is 19.5 mm and event is observed 20 minutes after construction began. Video is in real time. **https** : //**youtu**.**be**/**PER** − **ZRzcZhw**

Video S4. X-ray time lapse video of an ant tower. Black dots refer to ants that have ingested a radiographic contrast medium. Video is sped up 125 times. **https** : //**youtu**.**be**/**PQrx$_{\mathbf{N}}$5D9OE**

Video S5. Time lapse video of the bottom of an ant tower. Ants form tunnels throughout the building process. Video is sped up 128 times. **https** : //**youtu**.**be**/**ZjZ4c$_{\mathbf{Z}}$6Gu0**

Bibliography

[1] DIRKS, J.-H. and FEDERLE, W., "Fluid-based adhesion in insects–principles and challenges," *Soft Matter*, vol. 7, no. 23, pp. 11047–11053, 2011.

[2] FOTY, R. A. and STEINBERG, M. S., "Cadherin-mediated cell-cell adhesion and tissue segregation in relation to malignancy," *International Journal of Developmental Biology*, vol. 48, pp. 397–410, 2004.

[3] DOUEZAN, S., GUEVORKIAN, K., NAOUAR, R., DUFOUR, S., CUVELIER, D., and BROCHARD-WYART, F., "Spreading dynamics and wetting transition of cellular aggregates," *Proceedings of the National Academy of Sciences*, vol. 108, no. 18, pp. 7315–7320, 2011.

[4] TENNENBAUM, M., LIU, Z., FERNANDEZ-NIEVES, A., and HU, D. L., "Fire ants cushion applied force through active rearrangements," *Under review*, 2015.

[5] BEAUNE, G., STIRBAT, T. V., KHALIFAT, N., COCHET-ESCARTIN, O., GARCIA, S., GURCHENKOV, V. V., MURRELL, M. P., DUFOUR, S., CUVELIER, D., and BROCHARD-WYART, F., "How cells flow in the spreading of cellular aggregates," *Proceedings of the National Academy of Sciences*, vol. 111, no. 22, pp. 8055–8060, 2014.

[6] MLOT, N. J., TOVEY, C. A., and HU, D. L., "Fire ants self-assemble into waterproof rafts to survive floods," *Proceedings of the National Academy of Sciences*, vol. 108, no. 19, pp. 7669–7673, 2011.

[7] PHONEKEO, S., MLOT, N., MONAENKOVA, D., HU, D. L., and TOVEY, C., "Fire ants assemble to build a tower of constant strength," *In preparation*, 2015.

[8] SHERRATT, J. and MURRAY, J., "Models of epidermal wound healing," *Proceedings of the Royal Societies of London*, vol. 241, no. 1300, pp. 29–36, 1990.

[9] SINGER, A. and CLARK, R., "Cutaneous wound healing," *New England Journal of Medicine*, vol. 341, no. 10, pp. 738–746, 1999. PMID: 10471461.

[10] ACKLAND, A. J., HANES, R., and COHEN, M., "Self assembly of a model multicellular organism resembling the dictyostelium slime molds," *Quantitative Biology*, 2007.

[11] ANDERSON, C., THERAULAZ, G., and DENEUBOURG, J.-L., "Self-assemblages in insect societies," *Insectes Sociaux*, vol. 49, no. 2, pp. 99–110, 2002.

[12] DORIGO, M., BIRATTARI, M., and STUTZLE, T., "Ant colony optimization: artificial ants as a computational intelligence technique," *IEEE Computational Intelligence Magazine*, vol. 1, no. 4, pp. 28–39, 2006.

[13] GARNIER, S., GAUTRAIS, J., and THERAULAZ, G., "The biological principles of swarm intelligence," *Swarm Intelligence*, vol. 1, no. 1, pp. 3–31, 2007.

[14] SEELEY, T. D., *Honeybee Democracy*. Princeton University Press, 2010.

[15] CAVAGNA, A., CIMARELLI, A., GIARDINA, I., PARISI, G., SANTAGATI, R., STEFANINI, F., and VIALE, M., "Scale-free correlations in starling flocks," *Proceedings of the National Academy of Sciences*, vol. 107, no. 26, pp. 11865–11870, 2010.

[16] CHAZELLE, B., "The convergence of bird flocking," *Journal of the ACM*, vol. 61, no. 4, 2014.

[17] KORB, J., "Thermoregulation and ventilation of termite mounds," *Naturwissenschaften*, vol. 90, pp. 212–219, 2003.

[18] FRANKS, N. R., "Thermoregulation in army ant bivouacs," *Physiological Entomology*, vol. 14, no. 4, pp. 397–404, 1989.

[19] HANSELL, M., *Built by animals*. Oxford University Press, 2007.

[20] BONABEAU, E., THERAULAZ, G., DENEUBOURG, J.-L., LIONI, A., LIBERT, F., SAUWENS, C., and PASSERA, L., "Dripping faucet with ants," *Physical Review E*, vol. 57, no. 5, p. 5904, 1998.

[21] THERAULAZ, G., BONABEAU, E., SAUWENS, C., DENEUBOURG, J.-L., LIONI, A., LIBERT, F., PASSERA, L., and SOLÉ, R., "Model of droplet dynamics in the argentine ant linepithema humile (mayr)," *Bulletin of Mathematical Biology*, vol. 63, no. 6, pp. 1079–1093, 2001.

[22] COUZIN, I. D., KRAUSE, J., FRANKS, N. R., and LEVIN, S. A., "Effective leadership and decision-making in animal groups on the move," *Nature*, vol. 433, no. 7025, pp. 513–516, 2005.

[23] BENI, G. and WANG, J., "Swarm intelligence in cellular robotic systems," in *Robots and Biological Systems: Towards a New Bionics?*, pp. 703–712, Springer, 1993.

[24] CAO, Y. U., FUKUNAGA, A. S., and KAHNG, A., "Cooperative mobile robotics: Antecedents and directions," *Autonomous robots*, vol. 4, no. 1, pp. 7–27, 1997.

[25] DORIGO, M., TRIANNI, V., AHIN, E., GRO, R., LABELLA, T. H., BALDASSARRE, G., NOLFI, S., DENEUBOURG, J.-L., MONDADA, F., and FLOREANO, D., "Evolving self-organizing behaviors for a swarm-bot," *Autonomous Robots*, vol. 17, no. 2-3, pp. 223–245, 2004.

[26] GROSS, R., BONANI, M., MONDADA, F., and DORIGO, M., "Autonomous self-assembly in swarm-bots," *Robotics, IEEE Transactions on*, vol. 22, no. 6, pp. 1115–1130, 2006.

[27] RUBENSTEIN, M., CORNEJO, A., and NAGPAL, R., "Programmable self-assembly in a thousand-robot swarm," *Science*, vol. 345, no. 6198, pp. 795–799, 2014.

[28] CAMAZINE, S., *Self-organization in biological systems*. Princeton University Press, 2003.

[29] ALLEE, W. C., "Animal aggregations," 1931.

[30] SAVAGE, T. S., "I. on the habits of the drivers? or visiting ants of west africa," *Transactions of the Royal Entomological Society of London*, vol. 5, no. 1, pp. 1–15, 1847.

[31] ANDERSON, C. and FRANKS, N. R., "Teamwork in animals, robots, and humans," *Advances in the Study of Behavior*, vol. 33, pp. 1–48, 2003.

[32] ASHBY, W. R., "Principles of the self-organizing dynamic system," *The Journal of general psychology*, vol. 37, no. 2, pp. 125–128, 1947.

[33] BONABEAU, E., THERAULAZ, G., DENEUBOURG, J.-L., ARON, S., and CAMAZINE, S., "Self-organization in social insects," *Trends in Ecology & Evolution*, vol. 12, no. 5, pp. 188–193, 1997.

[34] COLORNI, A., DORIGO, M., MANIEZZO, V., and OTHERS, "Distributed optimization by ant colonies," in *Proceedings of the first European conference on artificial life*, vol. 142, pp. 134–142, Paris, France, 1991.

[35] HALLEY, J., WINKLER, D. A., and OTHERS, "Consistent concepts of self-organization and self-assembly," *Complexity*, vol. 14, no. 2, pp. 10–17, 2008.

[36] HÖLLDOBLER, B. and WILSON, E. O., *The superorganism: the beauty, elegance, and strangeness of insect societies*. WW Norton & Company, 2009.

[37] SUMPTER, D. J., "The principles of collective animal behaviour," *Philosophical Transactions of the Royal Society B: Biological Sciences*, vol. 361, no. 1465, pp. 5–22, 2006.

[38] HÖLLDOBLER, B. and WILSON, E. O., *The ants*. Harvard University Press, 1990.

[39] FRANKS, N. R. and RICHARDSON, T., "Teaching in tandem-running ants," *Nature*, vol. 439, no. 7073, pp. 153–153, 2006.

[40] MÖGLICH, M., MASCHWITZ, U., and HÖLLDOBLER, B., "Tandem calling: a new kind of signal in ant communication," *Science*, vol. 186, no. 4168, pp. 1046–1047, 1974.

[41] COUZIN, I. D. and FRANKS, N. R., "Self-organized lane formation and optimized traffic flow in army ants," *Proceedings of the Royal Society of London B: Biological Sciences*, vol. 270, no. 1511, pp. 139–146, 2003.

[42] DORIGO, M., BONABEAU, E., and THERAULAZ, G., "Ant algorithms and stigmergy," *Future Generation Computer Systems*, vol. 16, no. 8, pp. 851–871, 2000.

[43] ROSENGREN, R. and FORTELIUS, W., "Ortstreue in foraging ants of theformica rufa grouphierarchy of orienting cues and long-term memory," *Insectes Sociaux*, vol. 33, no. 3, pp. 306–337, 1986.

[44] COLLETT, T. S., GRAHAM, P., HARRIS, R. A., and HEMPEL-DE-IBARRA, N., "Navigational memories in ants and bees: memory retrieval when selecting and following routes," *Advances in the Study of Behavior*, vol. 36, p. 123, 2006.

[45] FEDERLE, W., RIEHLE, M., CURTIS, A. S., and FULL, R. J., "An integrative study of insect adhesion: mechanics and wet adhesion of pretarsal pads in ants," *Integrative and Comparative Biology*, vol. 42, no. 6, pp. 1100–1106, 2002.

[46] DIRKS, J.-H., CLEMENTE, C. J., and FEDERLE, W., "Insect tricks: two-phasic foot pad secretion prevents slipping," *Journal of The Royal Society Interface*, p. rsif20090308, 2009.

[47] DRECHSLER, P. and FEDERLE, W., "Biomechanics of smooth adhesive pads in insects: influence of tarsal secretion on attachment performance," *Journal of Comparative Physiology A*, vol. 192, no. 11, pp. 1213–1222, 2006.

[48] LIPP, A., WOLF, H., and LEHMANN, F.-O., "Walking on inclines: energetics of locomotion in the ant camponotus," *Journal of Experimental Biology*, vol. 208, no. 4, pp. 707–719, 2005.

[49] FOSTER, P. C., MLOT, N. J., LIN, A., and HU, D. L., "Fire ants actively control spacing and orientation within self-assemblages," *The Journal of experimental biology*, vol. 217, no. 12, pp. 2089–2100, 2014.

[50] GRAVISH, N., FRANKLIN, S. V., HU, D. L., and GOLDMAN, D. I., "Entangled granular media," *Physical review letters*, vol. 108, no. 20, p. 208001, 2012.

[51] FRANKLIN, S. V., "Extensional rheology of entangled granular materials," *EPL (Europhysics Letters)*, vol. 106, no. 5, p. 58004, 2014.

[52] MLOT, N. J., TOVEY, C. A., and HU, D. L., "Dynamics and shape of large fire ant rafts," *Communicative and Integrative Biology*, vol. 5, no. 6, pp. 590–597, 2012.

[53] CHEN, J., "Advancement on techniques for the separation and maintenance of the red imported fire ant colonies," *Insect science*, vol. 14, no. 1, pp. 1–4, 2007.

[54] DIRKS, J. H., CLEMENTE, C. J., and FEDERLE, W., "Insect tricks: two-phasic foot pad secretion prevents slipping," *Journal of The Royal Society Interface*, vol. 7, no. 45, pp. 587–593, 2010.

[55] FEDERLE, W., RIEHLE, M., CURTIS, A. S., and FULL, R. J., "An integrative study of insect adhesion: mechanics and wet adhesion of pretarsal pads in ants," *Integrative and Comparative Biology*, vol. 42, no. 6, pp. 1100–1106, 2002.

[56] TIMOSHENKO, S. P., *Strength of Materials*. D. Van Nostrand Company, 1930.

[57] SOLE, J. B., *L'Origen Dels Castells: Analisi Tecnica I Historica*. Cossetania, 2007.

[58] SCOTT, G., "Le siege de port-arthur-le pyramide humaine," *L'illustration*, vol. 62, no. 32, 1904.

[59] SCULLY, J., "Castellers of vilafranca make history creating the highest human tower of all time," *Catalan News Agency*, 2013.

[60] FELLER, W., *An Introduction to Probability Theory and Its Applications*, vol. II. John Wiley and Sons, 1971.

[61] GARNIER, S., MURPHY, T., LUTZ, M., HUME, E., LEGLANC, S., and AIN D. COUZIN, "Stability and responsiveness in a self-organizing living architecture," *PLoS Computational Biology*, vol. 9, no. 3, pp. 4–10, 2013.

[62] FRANKS, N. R., "Reproduction, foraging efficiency and worker polymorphism in army ants," *Experimental Behavioral and Sociobiology*, vol. 31, pp. 81–108, 1985.

[63] POWELL, S. and FRANKS, N. R., "How a few help all: living pothole plugs speed prey delivery in the army ant eciton burchellii," *Animal Behaviour*, pp. 1067–1076, 2006.

[64] LATANE, B., WILLIAMS, K., and HARKINS, S., "Many hands make light the work: The causes and consequences of social loafing.," *Journal of personality and social psychology*, vol. 37, no. 6, p. 822, 1979.

[65] MEHDIABADI, N. J., JACK, C. N., FARNHAM, T. T., PLATT, T. G., KALLA, S. E., SHAULSKY, G., QUELLER, D. C., and STRASSMANN, J. E., "Social evolution: kin preference in a social microbe," *Nature*, vol. 442, no. 7105, pp. 881–882, 2006.

[66] CUI, Z., WILLINGHAM, M. C., HICKS, A. M., ALEXANDER-MILLER, M. A., HOWARD, T. D., HAWKINS, G. A., MILLER, M. S., WEIR, H. M., DU, W., and DELONG, C. J., "Spontaneous regression of advanced cancer: identification of a

unique genetically determined, age-dependent trait in mice," *Proceedings of the National Academy of Sciences*, vol. 100, no. 11, pp. 6682–6687, 2003.

[67] BIBETTE, J., CHU, L.-Y., CARRERAS, E. S., ROYERE, A., and BREMOND, N., "Method for manufacturing capsule series, and related capsule series," Dec. 1 2009. US Patent App. 13/131,971.

[68] ALESSANDRI, K., SARANGI, B. R., GURCHENKOV, V. V., SINHA, B., KIESSLING, T. R., FETLER, L., RICO, F., SCHEURING, S., LAMAZE, C., SIMON, A., and OTHERS, "Cellular capsules as a tool for multicellular spheroid production and for investigating the mechanics of tumor progression in vitro," *Proceedings of the National Academy of Sciences*, vol. 110, no. 37, pp. 14843–14848, 2013.

[69] HIGGINS, C. A., CHEN, J. C., CERISE, J. E., JAHODA, C. A., and CHRISTIANO, A. M., "Microenvironmental reprogramming by three-dimensional culture enables dermal papilla cells to induce de novo human hair-follicle growth," *Proceedings of the National Academy of Sciences*, vol. 110, no. 49, pp. 19679–19688, 2013.

[70] TOYOSHIMA, K.-E., ASAKAWA, K., ISHIBASHI, N., TOKI, H., OGAWA, M., HASEGAWA, T., IRIÉ, T., TACHIKAWA, T., SATO, A., TAKEDA, A., and OTHERS, "Fully functional hair follicle regeneration through the rearrangement of stem cells and their niches," *Nature communications*, vol. 3, p. 784, 2012.

[71] CAO, Y., VACANTI, J. P., PAIGE, K. T., UPTON, J., and VACANTI, C. A., "Transplantation of chondrocytes utilizing a polymer-cell construct to produce tissue-engineered cartilage in the shape of a human ear," *Plastic and reconstructive surgery*, vol. 100, no. 2, pp. 297–302, 1997.

[72] LANCASTER, M. A., RENNER, M., MARTIN, C.-A., WENZEL, D., BICKNELL, L. S., HURLES, M. E., HOMFRAY, T., PENNINGER, J. M., JACKSON, A. P., and

KNOBLICH, J. A., "Cerebral organoids model human brain development and microcephaly," *Nature*, vol. 501, no. 7467, pp. 373–379, 2013.

[73] DUNHAM, L. J. and STEWART, H. L., "A survey of transplantable and transmissible animal tumors," *Journal of the National Cancer Institute*, vol. 13, no. 5, p. 1299, 1953.

[74] BOYER, B., DUFOUR, S., and THIERY, J. P., "E-cadherin expression during the acidic fgf-induced dispersion of a rat bladder carcinoma cell line," *Experimental cell research*, vol. 201, no. 2, pp. 347–357, 1992.

[75] PIMENTEL, D., ZUNIGA, R., and MORRISON, D., "Update on the environmental and economic costs associated with alien-invasive species in the united states," *Ecological economics*, vol. 52, no. 3, pp. 273–288, 2005.

[76] MACKAY, W. P., MAJDI, S., IRVING, J., VINSON, S. B., and MESSER, C., "Attraction of ants (hymenoptera: Formicidae) to electric fields," *Journal of the Kansas entomological society*, pp. 39–43, 1992.

[77] YIM, M., SHEN, W.-M., SALEMI, B., RUS, D., MOLL, M., LIPSON, H., KLAVINS, E., and CHIRIKJIAN, G. S., "Modular self-reconfigurable robot systems [grand challenges of robotics]," *Robotics & Automation Magazine, IEEE*, vol. 14, no. 1, pp. 43–52, 2007.

[78] PFEIFER, R., LUNGARELLA, M., and IIDA, F., "Self-organization, embodiment, and biologically inspired robotics," *Science*, vol. 318, no. 5853, pp. 1088–1093, 2007.

[79] WELLS, R. G., "The role of matrix stiffness in regulating cell behavior," *Hepatology*, vol. 47, no. 4, pp. 1394–1400, 2008.

[80] KIM, W., GILET, T., and BUSH, J. W., "Optimal concentrations in nectar feeding," *Proceedings of the National Academy of Sciences*, vol. 108, no. 40, pp. 16618–16621, 2011.

[81] FOTY, R. A., PFLEGER, C. M., FORGACS, G., and STEINBERG, M. S., "Surface tensions of embryonic tissues predict their mutual envelopment behavior," *Development*, vol. 122, no. 5, pp. 1611–1620, 1996.

[82] FORGACS, G., FOTY, R. A., SHAFRIR, Y., and STEINBERG, M. S., "Viscoelastic properties of living embryonic tissues: a quantitative study," *Biophysical Journal*, vol. 74, no. 5, pp. 2227–2234, 1998.

[83] MARTIN, I., DOZIN, B., QUARTO, R., CANCEDDA, R., and BELTRAME, F., "Computer-based technique for cell aggregation analysis and cell aggregation in in vitro chondrogenesis," *Cytometry*, vol. 28, no. 2, pp. 141–146, 1997.

[84] STEINBERG, M. S., "Reconstruction of tissues by dissociated cells. some morphogenetic tissue movements and the sorting out of embryonic cells may have a common explanation," *Science*, vol. 141, no. 3579, pp. 401–8, 1963. Steinberg, m s Journal Article Not Available Science. 1963 Aug 2;141(3579):401-8.

[85] STEINBERG, M. S., "Differential adhesion in morphogenesis: a modern view," *Current opinion in genetics & development*, vol. 17, no. 4, pp. 281–286, 2007.

[86] FOTY, R. A., FORGACS, G., PFLEGER, C. M., and STEINBERG, M. S., "Liquid properties of embryonic tissues: measurement of interfacial tensions," *Physical review letters*, vol. 72, no. 14, p. 2298, 1994.

[87] GUEVORKIAN, K., COLBERT, M.-J., DURTH, M., DUFOUR, S., and BROCHARD-WYART, F., "Aspiration of biological viscoelastic drops," *Physical review letters*, vol. 104, no. 21, p. 218101, 2010.

[88] SOLON, J., KAYA-COPUR, A., COLOMBELLI, J., and BRUNNER, D., "Pulsed forces timed by a ratchet-like mechanism drive directed tissue movement during dorsal closure," *Cell*, vol. 137, no. 7, pp. 1331–1342, 2009.

[89] LE PENNEC, T., MLY, K. J., HANSEN, A., AMMI, M., BIDEAU, D., and WU, X.-L., "Ticking hour glasses: experimental analysis of intermittent flow," *Physical Review E*, vol. 53, no. 3, p. 2257, 1996.

[90] BROCHARD, F. and DE GENNES, P., "Shear-dependent slippage at a polymer/solid interface," *Langmuir*, vol. 8, no. 12, pp. 3033–3037, 1992.

[91] MIGLER, K., HERVET, H., and LEGER, L., "Slip transition of a polymer melt under shear stress," *Physical review letters*, vol. 70, no. 3, p. 287, 1993.

[92] LINN, F. C., "Lubrication of animal joints," *The Journal of Bone & Joint Surgery*, vol. 49, no. 6, pp. 1079–1098, 1967.

[93] DAI, Z. and GORB, S. N., "Micro-structure and frictional characteristics of beetles joint," *Science in China Series G: Physics, Mechanics and Astronomy*, vol. 47, no. 1, pp. 99–106, 2004.

[94] DOUEZAN, S. and BROCHARD-WYART, F., "Spreading dynamics of cellular aggregates confined to adhesive bands," *The European Physical Journal E*, vol. 35, no. 11, pp. 1–6, 2012.

[95] JOHN, A., SCHADSCHNEIDER, A., CHOWDHURY, D., and NISHINARI, K., "Trafficlike collective movement of ants on trails: Absence of a jammed phase," *Physical review letters*, vol. 102, no. 10, p. 108001, 2009.

[96] NICOLIS, S. C., FERNNDEZ, J., PREZ-PENICHET, C., NODA, C., TEJERA, F., RAMOS, O., SUMPTER, D. J., and ALTSHULER, E., "Foraging at the edge of chaos:

internal clock versus external forcing," *Physical review letters*, vol. 110, no. 26, p. 268104, 2013.

[97] NICOLIS, S. C., REYES, A., and ALTSHULER, E., "Uninformed sacrifice: foraging ants do not cooperate against abduction," *Animal Behavior*, 2015.

[98] FERNÁNDEZ, J., TEJERA, F., REYES, A., and ALTSHULER, E., "Untitled," *Unpulished*, 2010.

[99] MONAENKOVA, D., GRAVISH, N., RODRIGUEZ, G., KUTNER, R., GOODISMAN, M. A., and GOLDMAN, D. I., "Behavioral and mechanical determinants of collective subsurface nest excavation," *The Journal of Experimental Biology*, vol. 218, no. 9, pp. 1295–1305, 2015.

[100] BALCH, T., KHAN, Z., and VELOSO, M., "Automatically tracking and analyzing the behavior of live insect colonies," *Proceedings of the fifth international conference on Autonomous agents*, pp. 521–528, 2001.

[101] KHAN, Z., BALCH, T., and DELLAERT, F., *An MCMC-based particle filter for tracking multiple interacting targets*, pp. 279–290. Springer, 2004.

[102] NODA, C., FERNÁNDEZ, J., PÉREZ-PENICHET, C., and ALTSHULER, E., "Measuring activity in ant colonies," *Review of scientific instruments*, vol. 77, no. 12, p. 126102, 2006.

[103] ROBINSON, E. J., RICHARDSON, T. O., SENDOVA-FRANKS, A. B., FEINERMAN, O., and FRANKS, N. R., "Radio tagging reveals the roles of corpulence, experience and social information in ant decision making," *Behavioral ecology and sociobiology*, vol. 63, no. 5, pp. 627–636, 2009.